

The retromer complex safeguards against neural progenitor-derived tumorigenesis by regulating Notch receptor trafficking

Bo Li^{1†}, Chouin Wong^{1†}, Shihong Max Gao¹, Rulan Zhang¹, Rongbo Sun^{2,3}, Yulong Li^{2,3,4}, Yan Song^{1,4*}

¹Ministry of Education Key Laboratory of Cell Proliferation and Differentiation, School of Life Sciences, Peking University, Beijing, China; ²State Key Laboratory of Membrane Biology, School of Life Sciences, Peking University, Beijing, China; ³PKU-IDG/McGovern Institute for Brain Research, Beijing, China; ⁴Peking-Tsinghua Center for Life Sciences, Peking University, Beijing, China

Abstract The correct establishment and maintenance of unidirectional Notch signaling are critical for the homeostasis of various stem cell lineages. However, the molecular mechanisms that prevent cell-autonomous ectopic Notch signaling activation and deleterious cell fate decisions remain unclear. Here we show that the retromer complex directly and specifically regulates Notch receptor retrograde trafficking in *Drosophila* neuroblast lineages to ensure the unidirectional Notch signaling from neural progenitors to neuroblasts. Notch polyubiquitination mediated by E3 ubiquitin ligase Itch/Su(dx) is inherently inefficient within neural progenitors, relying on retromer-mediated trafficking to avoid aberrant endosomal accumulation of Notch and cell-autonomous signaling activation. Upon retromer dysfunction, hypo-ubiquitinated Notch accumulates in Rab7⁺ enlarged endosomes, where it is ectopically processed and activated in a ligand-dependent manner, causing progenitor-originated tumorigenesis. Our results therefore unveil a safeguard mechanism whereby retromer retrieves potentially harmful Notch receptors in a timely manner to prevent aberrant Notch activation-induced neural progenitor dedifferentiation and brain tumor formation.

DOI: <https://doi.org/10.7554/eLife.38181.001>

*For correspondence:
yan.song@pku.edu.cn

†These authors contributed
equally to this work

Competing interests: The
authors declare that no
competing interests exist.

Funding: See page 22

Received: 08 May 2018

Accepted: 17 August 2018

Published: 04 September 2018

Reviewing editor: Thomas
Vaccari, , Italy

© Copyright Li et al. This article
is distributed under the terms of
the [Creative Commons
Attribution License](https://creativecommons.org/licenses/by/4.0/), which
permits unrestricted use and
redistribution provided that the
original author and source are
credited.

Introduction

The correct establishment and maintenance of unidirectional Notch signaling are critical for the homeostasis of various stem cell lineages (Bertet et al., 2014; Blanpain et al., 2006; Bowman et al., 2008; Conboy and Rando, 2002; Fre et al., 2005; Guo and Ohlstein, 2015; Lin et al., 2012; Liu et al., 2017; Ohlstein and Spradling, 2007; Ren et al., 2018; Song and Lu, 2011; Williams et al., 2011). The canonical Notch signaling, which requires two adjacent cells to present transmembrane ligands and transmembrane receptors respectively (Bray, 2006; Kopan and Ilagan, 2009) and involves intercellular or intracellular amplification step(s) to establish its unidirectionality (Artavanis-Tsakonas et al., 1999; Liu et al., 2017; Losick and Desplan, 2008), is an ideal signaling pathway for binary cell fate specification. Accordingly, Notch signaling has been implicated in cell fate decision-making events in diverse stem cell lineages (Bertet et al., 2014; Chen et al., 2016; Demitrack et al., 2015; Dong et al., 2012; Hilton et al., 2008; Homem and Knoblich, 2012; Liu et al., 2010; Ohlstein and Spradling, 2007; Pinto-Teixeira et al., 2018; Watt et al., 2008).

An important strategy utilized by dividing stem cells or progenitors to ensure binary cell fate decisions is asymmetric segregation of the endocytic protein Numb, an evolutionarily conserved Notch signaling antagonist, to one of the daughter cells (Bultje et al., 2009; Conboy and Rando, 2002;

eLife digest Most cells in the animal body are tailored to perform particular tasks, but stem cells have not yet made their choice. Instead, they have unlimited capacity to divide and, with the right signals, they can start to specialize to become a given type of cells. In the brain, this process starts with a stem cell dividing. One of the daughters will remain a stem cell, while the other, the neural progenitor, will differentiate to form a mature cell such as a neuron. Keeping this tight balance is crucial for the health of the organ: if the progenitor reverts back to being a stem cell, there will be a surplus of undifferentiated cells that can lead to a tumor.

A one-way signal driven by the protein Notch partly controls the distinct fates of the two daughter cells. While the neural progenitor carries Notch at its surface, its neural stem cell sister has a Notch receptor on its membrane instead. This ensures that the Notch signaling goes in one direction, from the cell with Notch to the one sporting the receptor.

When a stem cell divides, one daughter gets more of a protein called Numb than the other. Numb pulls Notch receptors away from the external membrane and into internal capsules called endosomes. This guarantees that only one of the siblings will be carrying the receptors at its surface. Yet, sometimes the Notch receptors can get activated in the endosomes, which may make neural progenitors revert to being stem cells. It is still unclear what tools the cells have to stop this abnormal activation.

Here, Li et al. screened brain cells from fruit fly larvae to find out the genes that might play a role in suppressing the inappropriate Notch signaling. This highlighted a protein complex known as the retromer, which normally helps to transport proteins in the cell. Experiments showed that, in progenitors, the retromer physically interacts with Notch receptors and retrieves them from the endosomes back to the cell surface. If the retromer is inactive, the Notch receptors accumulate in the endosomes, where they can be switched on. It seems that, in fruit flies, the retromer acts as a bomb squad that recognizes and retrieves potentially harmful Notch receptors, thereby preventing brain tumor formation.

Several retromer components are less present in patients with various cancers, including glioblastoma, an aggressive form of brain cancer. The results by Li et al. may therefore shed light on the link between the protein complex and the emergence of the disease in humans.

DOI: <https://doi.org/10.7554/eLife.38181.002>

Gunage et al., 2014; Lu et al., 1998; Luo et al., 2005; Rhyu et al., 1994; Sallé et al., 2017; Shen et al., 2002; Wang et al., 2006; Wu et al., 2017; Zhong et al., 1996). Numb acts as an adaptor to bridge the Notch receptor and its cofactor(s) with the endocytic machinery and reduces the surface pool of Notch by promoting its endocytosis (*Hutterer and Knoblich, 2005; Song and Lu, 2012*). Endocytosed Notch receptors are often poly-ubiquitinated by E3 ubiquitin ligases, such as Itch/Su(dx) (Suppressor of deltex) and Nedd4 (*Cornell et al., 1999; Le Bras et al., 2011; Qiu et al., 2000; Sakata et al., 2004; Wilkin et al., 2004*), and sorted through the ESCRT (Endosomal Sorting Complex Required for Transport) pathway for lysosomal degradation (*Horner et al., 2018; Thompson et al., 2005; Vaccari et al., 2009*). As a consequence, the daughter cell inheriting relatively more Numb protein becomes the Notch signaling sending cell, unambiguously establishing signaling directionality. Not surprisingly, dysregulation in the asymmetric segregation of Numb has been implicated in a wide range of developmental defects and diseases (*Bowman et al., 2008; Bu et al., 2016; Caussin and Gonzalez, 2005; George et al., 2013; Li et al., 2003; Pece et al., 2004*).

However, the plasma membrane is not the only location where the Notch receptor can be processed and activated. The proteolytic activity of γ -secretase has been detected in endosomal membranes (*Gupta-Rossi et al., 2004; Lah and Levey, 2000; Pasternak et al., 2003; Urra et al., 2007*). Furthermore, it has been postulated that the relatively low pH at the endosomal compartments renders a conformational change in the Notch receptor, allowing for more efficient proteolysis. Indeed, inactivation of the ESCRT complex leads to retention of the Notch receptor in the limiting membrane of multivesicular bodies (MVBs) where Notch is ectopically activated via ligand-independent, γ -secretase-dependent proteolysis (*Hori et al., 2011; Thompson et al., 2005; Vaccari and Bilder,*

2005; Vaccari et al., 2009; Wilkin et al., 2008; Zhou et al., 2016). Other than ESCRT pathway-mediated lysosomal degradation, how protein trafficking machinery prevents deleterious cell-autonomous Notch signaling activation in stem cell lineages remains to be elucidated.

Type II neural stem cells, so called neuroblasts, in the *Drosophila* larval central brain region provide an attractive model system for studying how endosomal trafficking establishes unidirectional Notch signaling and ensures stem cell versus progenitor binary cell fate decisions (Figure 1A) (Liu et al., 2017; Song and Lu, 2012). Firstly, type II neural stem cell lineages resemble their mammalian counterparts in terms of regulatory molecules and principles, yet with much simpler anatomical structure and lineage composition (Brand and Livesey, 2011; Homem and Knoblich, 2012; Sousa-Nunes et al., 2010). Secondly, unidirectional Notch signaling is critical for establishing type II neuroblast versus immature intermediate neural progenitor (INP) binary cell fates (Bowman et al., 2008; Song and Lu, 2011; Song and Lu, 2012; Wang et al., 2006; Weng et al., 2010). Whereas downregulation of Notch signaling in neuroblasts leads to their premature differentiation into INPs and loss of stemness, overactivation of Notch signaling in neural progenitors cause their fate reversion back into neuroblast-like state and tumorigenesis (Bowman et al., 2008; Song and Lu, 2011; Song and Lu, 2012; Wang et al., 2006; Weng et al., 2010). Thus, the total number of neuroblasts in each brain lobe represents a quantitative and precise readout of Notch signaling strength. Thirdly, Numb is asymmetrically inherited by immature INPs, where it dampens Notch signaling partly by reducing the cell surface pool of mature Notch receptors (Figure 1B) (Bowman et al., 2008; Lee et al., 2006b; Song and Lu, 2012; Wang et al., 2006).

In a large-scale unbiased RNAi-based genetic screen for regulators of neuroblast versus progenitor cell fate decision, we identified Vps26, a subunit of the retromer complex (Burd and Cullen, 2014; Wang and Bellen, 2015). Specific downregulation of Vps26 in *Drosophila* central brain neuroblast lineages led to a supernumerous neuroblast phenotype. The retromer complex is an evolutionarily highly conserved endosomal sorting complex, which plays a crucial role in the retrograde trafficking of a specific subset of endocytosed proteins from endosomes back to the trans-Golgi network or the plasma membrane (Burd and Cullen, 2014; Wang and Bellen, 2015). The core of the retromer complex is a vacuolar protein sorting (Vps) trimer composed of Vps35, Vps26 and Vps29 subunits (Figure 1C). Previous studies have implicated retromer in controlling a wide range of physiological processes, such as regulating fly wing development, maintaining the function of photoreceptors, establishing cell polarity in epithelial cells, controlling LTP (long-term potential) in mature hippocampus, modulating fly oogenesis and propagating mitochondrial stress signals (Belenkaya et al., 2008; Chen et al., 2010; Choy et al., 2014; Coudreuse et al., 2006; Franch-Marro et al., 2008; Gomez-Lamarca et al., 2015; Harterink et al., 2011; Hesketh et al., 2014; Pan et al., 2008; Pocha et al., 2011; Port et al., 2008; Starble and Pokrywka, 2018; Temkin et al., 2011; Temkin et al., 2017; Wang and Bellen, 2015; Yang et al., 2008; Zhang et al., 2018). Dysfunction of retromer-mediated endosomal sorting has been linked to various pathologies, including neurodegenerative diseases such as Alzheimer's disease and Parkinson's disease (McMillan et al., 2017; Small and Petsko, 2015; Wang and Bellen, 2015).

Here our results unveil a safeguard mechanism through which the retromer complex ensures sufficient dampening of Notch signaling in neural progenitors. Upon attenuation of the retromer function, hypo-ubiquitinated Notch that fails to enter the ESCRT-lysosomal pathway accumulates in enlarged Rab7⁺ endosomes and is ectopically processed and activated. Such cell-autonomous intracellular hyperactivation of Notch signaling causes fate reversion of neural progenitors and the formation of transplantable tumors. These results led us to propose a model whereby retromer serves as 'bomb squad' to retrieve and disarm the potentially harmful pool of Notch receptors in a timely manner.

Results

The retromer complex prevents neural progenitor dedifferentiation and tumorigenesis

To investigate the function of retromer in neuroblast lineages, we first downregulated Vps26 in all central brain neuroblast lineages using short hairpin microRNAs (shmiRNAs), driven by *insc-Gal4*, and observed a supernumerary neuroblast phenotype (Figure 1D,E). Such brain tumor phenotype

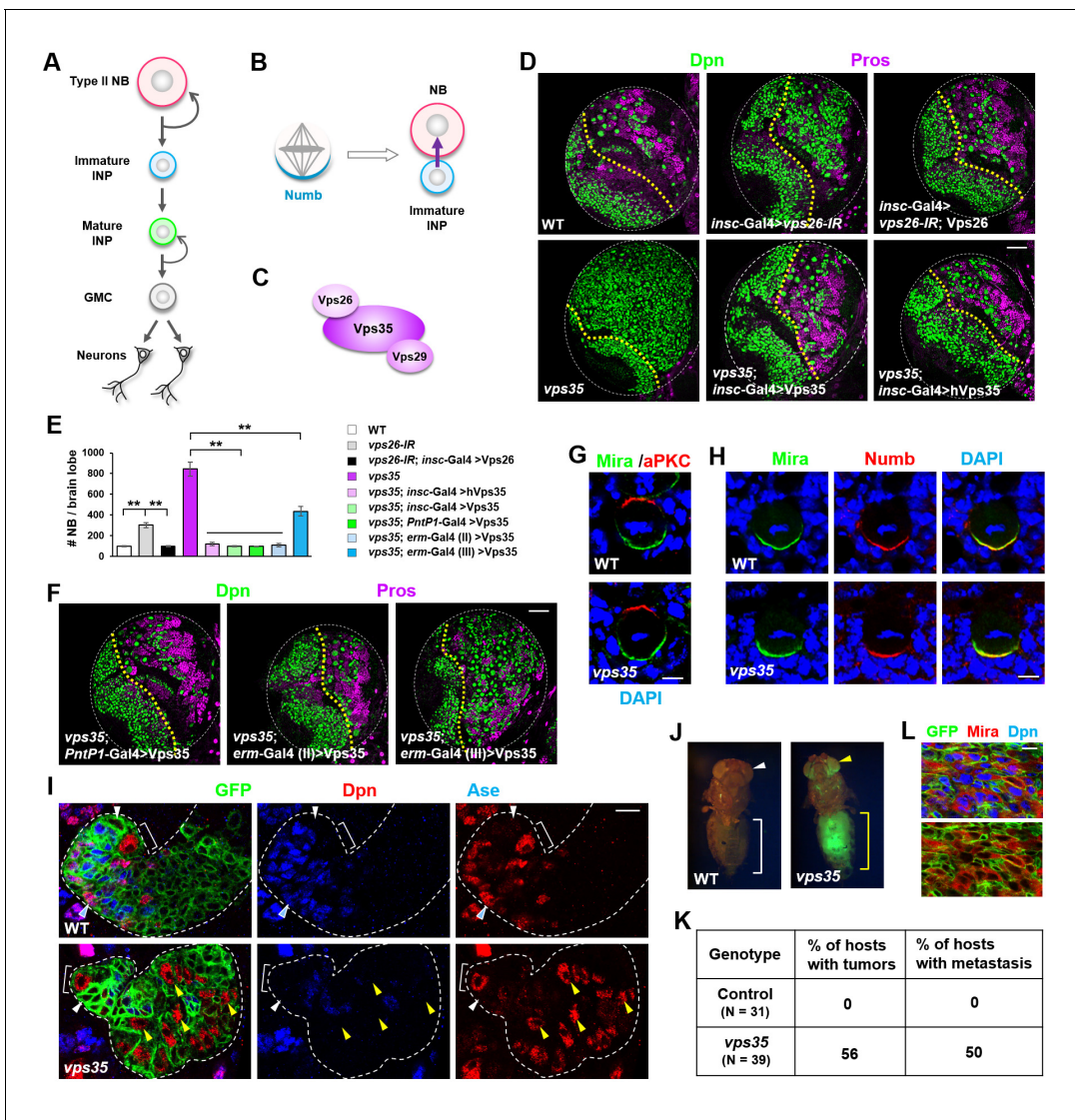


Figure 1. Dedifferentiation of *vps35* mutant neural progenitors causes the formation of transplantable tumors. (A) Diagram depicting the lineage hierarchy of *Drosophila* type II neuroblasts in the central brain area. (B) Schematic showing how asymmetric distribution and segregation of the endocytic protein Numb (cyan) initiates unidirectional Notch signaling (purple arrow) from a neural progenitor (light blue) to its sibling type II neuroblast (pink). (C) Schematic of the cargo-recognition retromer complex. (D–F) Larval brain lobes of indicated genotypes were stained for neuroblast marker Deadpan (Dpn) and ganglion mother cell (GMC)/neuronal marker Prospero (nuclear Pros) (D,F). In this and subsequent micrographs, yellow dotted line marks the boundary between the optic lobe (left) and the central brain (right) areas. Quantification of total neuroblast number per brain lobe is shown in (E). ** $p < 0.001$ ($n = 12–16$). (G) Asymmetric cortical distribution of apical marker atypical PKC (aPKC) and basal marker Miranda (Mira) in wild type (WT) or *vps35* mutant metaphase neuroblasts. (H) Colocalization of Mira and cell fate determinant Numb at the basal cortex of WT or *vps35* mutant metaphase neuroblasts. (I) MARCM clonal analysis of type II neuroblast lineages in WT control or *vps35* mutant backgrounds. In this and subsequent micrographs, type II neuroblast MARCM clones are marked by CD8-GFP and outlined by white dashed lines, whereas neuroblasts, immature intermediate neural progenitors (INPs), mature INPs and neuroblast-like dedifferentiating progenitors are marked with brackets, white arrowheads, cyan arrowheads and yellow arrowheads respectively. (J) Transplantation of GFP⁺ tissue from WT control larval brains into the abdomens of adult host flies caused neither tumorous growth (while bracket) nor metastasis (white arrowhead). In sharp contrast, transplantation of GFP⁺ tumor tissue from *vps35* mutant larval brains caused massive tumor formation (yellow bracket) and metastasis to distal organs such as the eyes (yellow arrowhead). (K) Table showing the frequency of tumor formation or metastasis 14 days after transplantation of GFP⁺ tissue from larval brains of indicated genotypes. (L) GFP⁺ tumor tissues from the transplanted hosts were isolated and stained for neuroblast markers Mira and Dpn. Note that most of the extracted GFP⁺ tumor cells were Mira⁺ and Dpn⁺ neuroblast-like cells. Scale bars, 50 μ m (D,F); 5 μ m (G,H) and 10 μ m (I,L).

DOI: <https://doi.org/10.7554/eLife.38181.003>

The following source data and figure supplements are available for figure 1:

Source data 1. Input data for bar graph **Figure 1E**.

Figure 1 continued on next page

Figure 1 continued

DOI: <https://doi.org/10.7554/eLife.38181.008>

Figure supplement 1. A summary of the Gal4 drivers and cell type markers used in this study.

DOI: <https://doi.org/10.7554/eLife.38181.004>

Figure supplement 2. Ectopic neuroblasts formed upon retromer dysfunction are originated from immature INPs.

DOI: <https://doi.org/10.7554/eLife.38181.005>

Figure supplement 3. MARCM clonal analysis of wild type and *vps35* mutant neuroblasts.

DOI: <https://doi.org/10.7554/eLife.38181.006>

Figure supplement 4. Lineage-tracing analysis of wild type and *vps35* mutant immature neural progenitors.

DOI: <https://doi.org/10.7554/eLife.38181.007>

induced by *vps26-RNAi* was fully rescued by the coexpression of a shmiRNA-resistant form of the Vps26 transgene, excluding the possibility of an off-target effect of the shmiRNA (**Figure 1D,E**). Furthermore, homozygous *vps35* mutant larval brains exhibited an even more severe supernumerary neuroblast phenotype than *vps26-IR*, and such phenotype was fully rescued upon specific expression of a Vps35 transgene in all central brain neuroblast lineages (**Figure 1D,E**). Importantly, human Vps35 also fully rescued the brain tumor phenotype of *vps35* mutants back to wild type (**Figure 1D,E**). Taken together, our results clearly indicated that retromer plays an evolutionarily-conserved role in preventing ectopic neuroblast formation in the central brain area.

To investigate the cellular origin of the ectopic neuroblasts formed upon retromer inactivation, we expressed the Vps35 transgene in distinct subset of cells within central brain neuroblast lineages and assessed its ability to rescue the *vps35* mutant phenotype. Expression of the Vps35 transgene in type II neuroblast lineages, by *PntP1-Gal4* (Zhu *et al.*, 2011), fully suppressed the brain tumor phenotype caused by *vps35* mutation (**Figure 1E,F** and **Figure 1—figure supplement 1**). By contrast, restoring Vps35 function in type I neuroblast lineages, by *ase-Gal4* (Zhu *et al.*, 2006), failed to do so (data not shown). These results indicated that the ectopic neuroblasts in retromer mutants are derived from type II neuroblast lineages. Indeed, expression of the Vps35 transgene in Deadpan (Dpn^- Ase $^-$) INPs by *erm-Gal4* (II) but not in Dpn^- Ase $^+$ INPs by *erm-Gal4* (III) (Pfeiffer *et al.*, 2008) completely rescued the supernumerary neuroblast phenotype caused by Vps35 inactivation (**Figure 1E,F** and **Figure 1—figure supplement 1**). Therefore, the reverting Dpn^- Ase $^-$ neural progenitors are the cellular origin of brain tumor in *vps35* mutants. Supporting this notion, cell polarity remained unaltered in *vps35* mutant neuroblasts (**Figure 1G**), indicating that these ectopic neuroblasts are not resulted from neuroblast symmetric division. Importantly, Numb is normally localized to the basal cortex of *vps35* mutant dividing neuroblasts (**Figure 1H**), arguing against the possibility that defective asymmetric segregation of Numb causes INP dedifferentiation in *vps35* mutant brains. Consistently, whereas Vps26 downregulation in type II neuroblast lineages or immature INP lineages, driven by *PntP1-Gal4* or *erm-Gal4*(II) respectively, resulted in supernumerary neuroblast phenotype, its knockdown in mature INP lineages or type I neuroblast lineages, driven by *erm-Gal4* (III) or *ase-Gal4* respectively, failed to induce ectopic neuroblasts (**Figure 1—figure supplement 2**). Furthermore, distinct from wild type control type II neuroblast MARCM clones (Lee and Luo, 1999) that contained one and only one Dpn^+ Ase $^-$ neuroblast (white bracket in **Figure 1I** and **Figure 1—figure supplement 1B**), *vps35* mutant clones contained multiple ectopic Dpn^+ Ase $^-$ Pros $^-$ neuroblast-like cells (yellow arrowheads in **Figure 1** and **Figure 1—figure supplement 3**) several cell diameters away from the primary neuroblast (white bracket in **Figure 1I**). These ectopic Dpn^+ Ase $^-$ Pros $^-$ neuroblast-like cells were of intermediate cell sizes between neural progenitors and primary neuroblasts (yellow arrowheads in **Figure 1** and **Figure 1—figure supplement 3**), indicating that they were undergoing dedifferentiation (Song and Lu, 2011). In addition, FLP-FRT-based lineage tracing by inducing GFP $^+$ clones exclusively in immature INPs, driven by *erm-Gal4* (II), resulted in labeling of INPs (white arrowhead in **Figure 1—figure supplement 4**), GMCs, and neurons (cyan arrowhead in **Figure 1—figure supplement 4**) in wild-type brains. In contrast, in *vps35* mutant brains, GFP-labeled ectopic type II neuroblasts of various cellular sizes were found after similar lineage tracing (yellow arrowheads in **Figure 1—figure supplement 4**), indicating that immature INPs could indeed dedifferentiate back into neuroblast-like cells upon retromer dysfunction. Taken together, our results clearly indicate that the brain tumor phenotype in *vps35* mutants is caused by cell fate reversion of Dpn^- Ase $^-$ neural progenitors.

We next employed transplantation assay to test whether the ectopic neuroblasts in *vps35* mutant brains are capable of initiating tumor. Transplantation of *vps35* mutant but not wild-type control brain tissues into the abdomens of host flies caused the formation of massive tumors (yellow bracket in **Figure 1J**) that often metastasize to distal organs (yellow arrowhead in **Figure 1J**; statistic results in **Figure 1K**). Importantly, the *vps35* mutant GFP⁺ tumor cells extracted from the abdomen of transplanted hosts were Dpn⁺ Miranda (Mira)⁺ neuroblast-like cells (**Figure 1L**). Thus *vps35* mutant cells in the larval brains are indeed tumor-initiating cells. Together, we conclude that retromer acts as a tumor suppressor in the *Drosophila* brain by preventing neural progenitor dedifferentiation.

***vps35* mutant dedifferentiating neural progenitors contained enlarged Rab7-positive endosomal vesicles**

Since the well-characterized function of retromer is retrograde transport of transmembrane proteins, we next assessed whether the distribution of any subcellular marker(s) is altered upon inactivation of retromer function. Compared to wild-type control INPs, *vps35* mutant INPs or ectopic neuroblasts displayed dramatically enlarged late endosomes/MVBs (**Figure 2A–C**; up to more than 10-fold increase in endosomal vesicle sizes). The expression levels of Rab7 remained unchanged in *vps35* mutants (**Figure 2D**), ruling out the likelihood that Vps35 regulates Rab7 gene expression or protein stability. Furthermore, Rab7 primarily colocalized with early endosome marker Rab5 in *vps35* but not

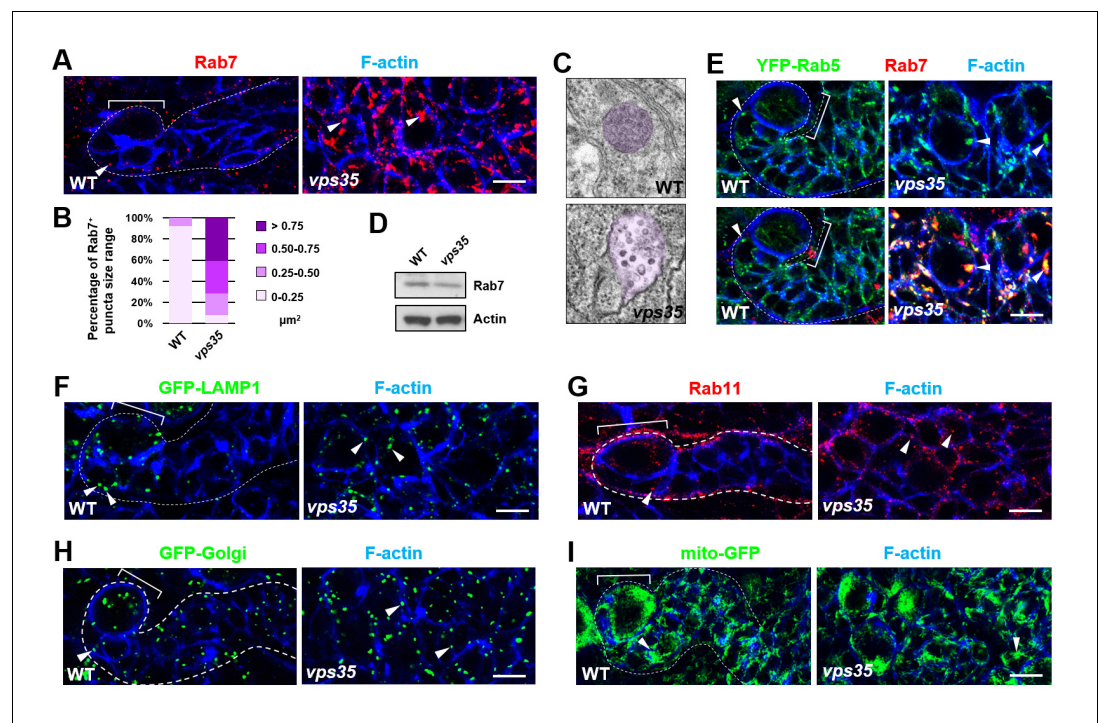


Figure 2. Rab7⁺ endosomes are drastically enlarged in *vps35* mutant neuroblast lineages. (A,B) Compared to WT control immature INPs, Rab7⁺ endosomes were dramatically enlarged in *vps35* mutant dedifferentiating neural progenitors (arrowheads in A). Quantification of the size range of Rab7⁺ puncta in immature INPs of indicated genotypes was shown in (B). (C) Transmission electron micrograph of wild type or *vps35* mutant larval brain neuroblasts. The mean size of MVBs, identified by the presence of intraluminal vesicles, was greatly enlarged in *vps35* mutant neuroblasts. Note that neuroblasts were identified by their large cellular and nuclear sizes and MVBs are highlighted in purple. (D) Western blot analysis of larval brain extracts of indicated genotypes using anti-Rab7 antibody. Anti-β-actin blot served as a loading control. (E) The enlarged Rab7⁺ endosomes in *vps35* mutant neuroblast-like cells were also positive for YFP-Rab5 (arrowheads). (F–I) Compared to WT control immature INPs, the sizes of GFP-LAMP1⁺ lysosomes (F), Rab11⁺ recycling endosomes (G), Golgi (H) or mitochondria marked by mito-GFP (I) remained unaltered in *vps35* mutant dedifferentiating neural progenitors (arrowheads). Scale bars, 10 μm (A, E–I).

DOI: <https://doi.org/10.7554/eLife.38181.009>

wild type cells (**Figure 2E**), demonstrating that the enlarged MVBs in *vps35* mutant cells are of early and late endosome hybrid identities. In contrast, other subcellular markers including lysosome (GFP-LAMP1), recycling endosome (Rab11), Golgi (GFP-Golgi) and mitochondria (mito-GFP) remained unchanged in *vps35*-defective cells (**Figure 2F–2I**). Therefore, our results strongly suggest that retromer normally functions in neural progenitors to transport cargo proteins away from early and late endosomes. Upon retromer dysfunction, its cargo proteins highly accumulate in MVBs, resulting in enlarged, aberrant endosomal vesicles of hybrid identities.

Retromer regulates retrograde trafficking of Notch receptors

We next sought to identify the critical cargo protein(s) of retromer in preventing INP dedifferentiation. Since Notch pathway is both necessary and sufficient to promote self-renewal in type II neuroblast lineages, we first examined the subcellular distribution of transmembrane protein components of Notch signaling pathway. We noted that the Notch receptor and its cofactor Sanpodo (*Couturier et al., 2012; Hutterer and Knoblich, 2005; O'Connor-Giles and Skeath, 2003; Song and Lu, 2012*) highly accumulated in enlarged puncta in *vps35* mutant cells, mostly colocalizing with Rab7⁺ enlarged endosomes (**Figure 3A,B** and **Figure 3—figure supplement 1**). In contrast, the distribution of other signaling molecules such as Patched (Ptc) and Wnt/Wingless (Wg) remained unaltered upon *Vps35* depletion (**Figure 3—figure supplement 2A–C**), indicating that retromer specifically mediates Notch receptor trafficking in neuroblast lineages. Strongly supporting this notion, Notch signaling reporter E(spl)mγ-GFP (*Almeida and Bray, 2005; Song and Lu, 2011*), which faithfully reflects Notch signaling activity in neuroblast lineages, was undetectable in wild type Dpn⁻ Ase⁻ immature INPs (white arrowhead in **Figure 3C**) but ectopically turned on in Dpn⁺ Ase⁻ dedifferentiating neural progenitors (yellow arrowhead in **Figure 3C**) upon *Vps26* downregulation. In addition, Notch puncta colocalizing with Rab7⁺ endosomes remained unaltered in *vps35* mutant wing imaginal disc epithelia (arrowheads in **Figure 3—figure supplement 2D**), suggesting a tissue-specific regulation of Notch trafficking by retromer. Collectively, retromer normally suppresses Notch activity through mediating retrograde trafficking of Notch receptors in neural progenitors.

We next assessed whether Notch is a crucial cargo of retromer in neuroblast lineages. Neuroblast lineage-specific knockdown of Notch completely suppressed the neuroblast overproliferation phenotype in *vps35* mutants (**Figure 3D,E**), indicating that the dedifferentiation process of *vps35* mutant INPs was Notch signaling-dependent. Type II neuroblast lineage-specific or immature INP-specific depletion of the ligand Delta, as well as neuroblast lineage-specific expression of a dominant negative form of Delta (*DI-DN*) that lacks its intracellular domain (*Baonza et al., 2000; Flores et al., 2000; Huppert et al., 1997*), completely or potentially suppressed brain tumor phenotypes caused by *vps35* mutations (**Figure 3D,E** and **Figure 3—figure supplement 2E,F**). Furthermore, type II neuroblast lineage-specific or immature INP-specific expression of a dominant negative form of the metalloprotease Kuzbanian (*Kuz-DN*), which lacks its protease activity and thereby specifically blocks ligand-induced S2 cleavage of Notch (*Lieber et al., 2002; Mumm et al., 2000; Pan and Rubin, 1997*), also phenocopied the effect of *Notch-RNAi* in inhibiting brain tumor formation (**Figure 3D,E**). These observations indicated that overactivation of Notch signaling in *vps35* mutant neural progenitors is largely, if not completely, ligand-dependent. Not surprisingly, a functional γ-secretase is also essential for ectopic activation of Notch signaling in *vps35* mutants (**Figure 3D,E**). In sharp contrast, inactivation of various other signaling pathways, such as Wnt/Wg, Hedgehog or EGFR, or overactivation of Hedgehog signaling showed no effects on the supernumerary neuroblast phenotype in *vps35* mutants (**Figure 3D,E** and **Figure 3—figure supplement 2E,F**), further demonstrating the high specificity of retromer on Notch signaling pathway in neuroblast lineages. Importantly, Notch colocalized with fly or human *Vps35* transgene (**Figure 3F,G**) and endogenous *Vps26* (**Figure 3H** and **Figure 3—figure supplement 3**). More remarkably, Notch depletion by RNAi led to a dramatic reduction in Rab7⁺ endosomal vesicle sizes almost back to normal (**Figure 3I**), suggesting that Notch receptors constitute the major endosomal contents of these aberrant *vps35* mutant vesicles. Taken together, our results strongly suggested that the Notch receptor is a functionally important cargo of retromer in type II neuroblast lineages.

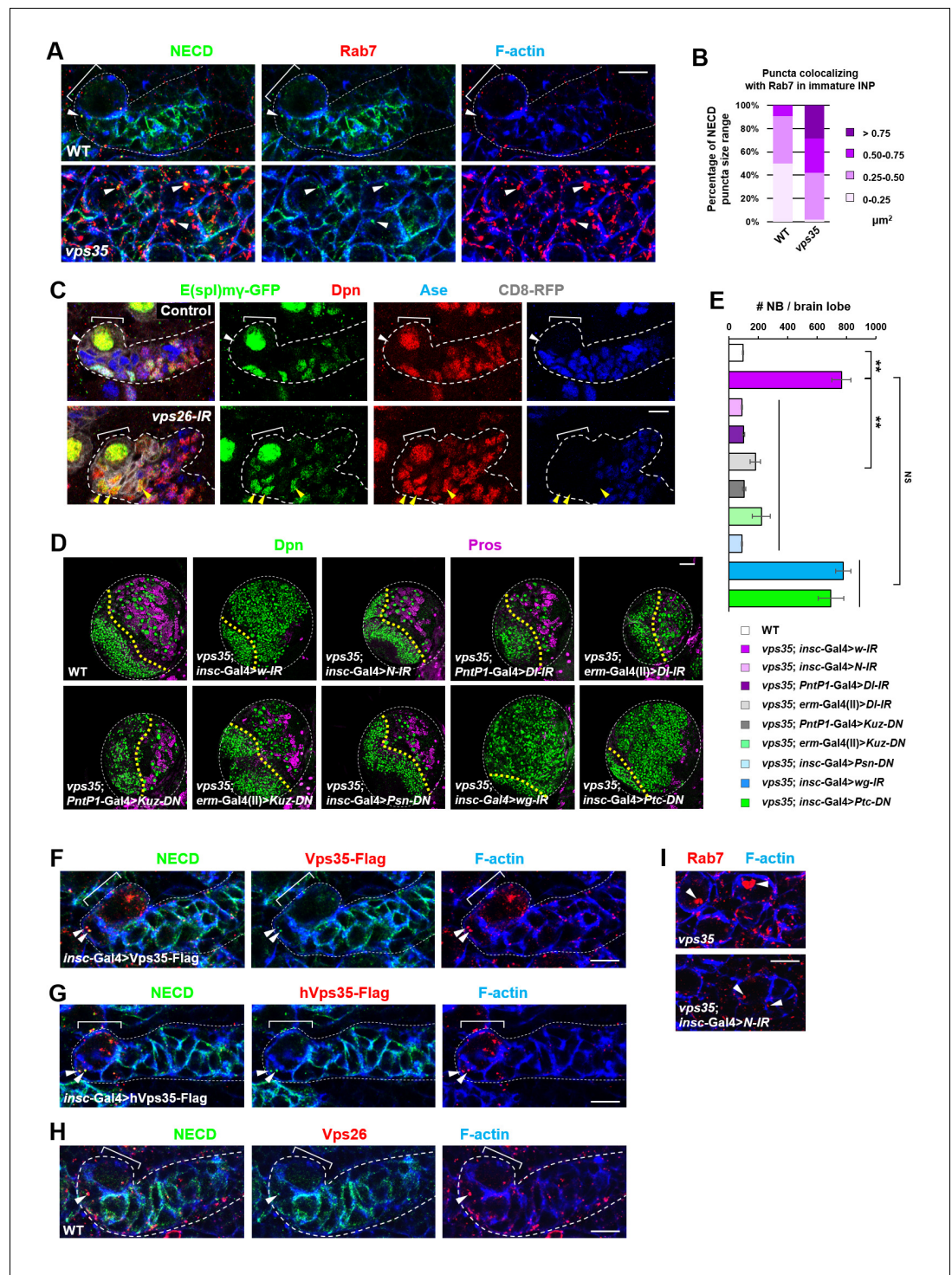


Figure 3. Retromer regulates Notch signaling by mediating Notch receptor endosomal trafficking. (A,B) Compared to WT control immature INPs, Notch puncta colocalizing with Rab7⁺ endosomes were enlarged in *vps35* mutant dedifferentiating neural progenitors (arrowheads in A). Quantification of the size range of Notch puncta colocalizing with Rab7⁺ endosomes is shown in (B). (C) The expression pattern of Notch signaling reporter E(spl)my-GFP in wild type control or *vps26-RNAi* type II neuroblast lineages. Note that immature INPs (Dpn⁻ Ase⁻) in control type II neuroblast lineages and dedifferentiating neural progenitors (Dpn⁺ Ase⁺) in *vps26-RNAi* lineages are marked with white arrowheads and yellow arrowheads respectively. (D,E) Larval brain lobes of indicated genotypes were stained for Dpn and Pros. Quantification of total neuroblast number per brain lobe is shown in (E). **p<0.001 (n = 10–18). NS, not significant. (F) Type II neuroblast lineages expressing Vps35-FLAG were stained for

Figure 3 continued on next page

Figure 3 continued

Notch extracellular domain (NECD) and FLAG. Note that NECD puncta (arrowheads) colocalized with Vps35-FLAG in immature INPs. (G,H) NECD puncta colocalized with FLAG-tagged human Vps35 (hVps35-FLAG; G) and endogenous Vps26 (H) in immature INPs (arrowheads). (I) Type II neuroblast lineages of indicated genotypes were stained for Rab7 and F-actin. Rab7 puncta are marked with arrowheads. Scale bars, 10 μm (A,C,F–I) and 50 μm (D). DOI: <https://doi.org/10.7554/eLife.38181.010>

The following source data and figure supplements are available for figure 3:

Source data 1. Input data for bar graph **Figure 3E**.

DOI: <https://doi.org/10.7554/eLife.38181.014>

Figure supplement 1. Retromer regulates endosomal trafficking of Notch cofactor Sanpodo (Spdo).

DOI: <https://doi.org/10.7554/eLife.38181.011>

Figure supplement 2. Retromer regulates Notch signaling in fly neuroblast lineages with high specificity.

DOI: <https://doi.org/10.7554/eLife.38181.012>

Figure supplement 3. Antibody raised against Vps26 is highly specific.

DOI: <https://doi.org/10.7554/eLife.38181.013>

Notch is a bona fide cargo protein of retromer

To validate that the Notch receptor is a cargo protein of the retromer complex, we assessed their physical interaction by performing coimmunoprecipitation (colP) assays. Vps35 or Vps26 was specifically coimmunoprecipitated with Notch intracellular domain (NICD) from HEK293T cell extracts (**Figure 4A**). Further domain mapping experiments revealed that the ankyrin repeat region but not the C-terminal region of NICD exhibited a strong binding activity to Vps26 (**Figure 4B,C**). Reciprocal colP assay showed that Vps26 utilized its middle domain to interact with NICD (**Figure 4D,E**). Furthermore, Notch-V5 expressed in central brain neuroblast lineages was specifically coimmunoprecipitated with Vps35-FLAG from fly larval brain extracts (**Figure 4F**), confirming the *in vivo* protein-protein interaction. Importantly, colP experiments further revealed interaction between mouse NICD and mouse Vps26 proteins (**Figure 4G,H**), indicating that the physical association between the retromer cargo-recognition complex and Notch is evolutionarily conserved. Taken together, our results validate that the Notch receptor is a bona fide cargo protein of the retromer complex.

Retromer prevents intracellular hyperactivation of Notch signaling

Our results presented so far support an intriguing possibility that the retromer complex physically interacts with Notch and transports it away from early and late endosomes in a timely and efficient manner. When retromer is defective, Notch receptors are trapped at early/late aberrant endosomal vesicles and is ectopically processed and activated, causing neural progenitor-derived brain tumor.

If this hypothesis is correct, one would expect that blocking the flux of Notch receptors towards its activating compartment or accelerating Notch trafficking away from it might prevent the accumulation and subsequent ectopic activation of Notch in *vps35* mutants (**Figure 5A**). Indeed, overexpression of a dominant negative form of Rab5 GTPase (*Rab5-DN*), which blocks the fusion of endocytic vesicles with early endosomes, or a constitutively active form of Rab9 GTPase (*Rab9-CA*), which promotes protein retrograde trafficking from late endosomes to trans-Golgi network (TGN) or the plasma membrane (**Figure 5—figure supplement 1**), completely suppressed brain tumor formation in *vps35* mutant brains (**Figure 5B,C**). Importantly, both the enlargement of Rab5/Rab7-positive endosomal vesicles and the high accumulation of Notch in these aberrant endosomal compartments in *vps35* mutant cells were effectively relieved upon *Rab5-DN* or *Rab9-CA* coexpression (arrowheads in **Figure 5D,E**). On the other hand, overexpression of a constitutively active form of Rab7 (*Rab7-CA*) or the ESCRT-0 complex component Hrs (Hepatocyte growth factor-regulated tyrosine kinase substrate), which accelerates the protein trafficking towards lysosome (**Figure 5—figure supplement 1**) (Lloyd *et al.*, 2002), potently inhibited the neuroblast overproliferation phenotype in *vps35* mutant brains (**Figure 5A,B,C**). Indeed, coexpression of either *Rab7-CA* or Hrs led to high accumulation of Notch in lysosomes of *vps35* mutant cells (**Figure 5F**). In contrast, overexpression of a constitutively active form of Rab5 GTPase (*Rab5-CA*), which accelerates the fusion of endocytic vesicles with early endosomes, or a dominant negative form of Rab7 (*Rab7-DN*) or Rab9 (*Rab9-DN*) GTPase, which prevents transport of proteins away from the sorting endosomes, failed to suppress the supernumerary neuroblast phenotype in *vps35* mutant brains (**Figure 5—figure supplement 2**). In

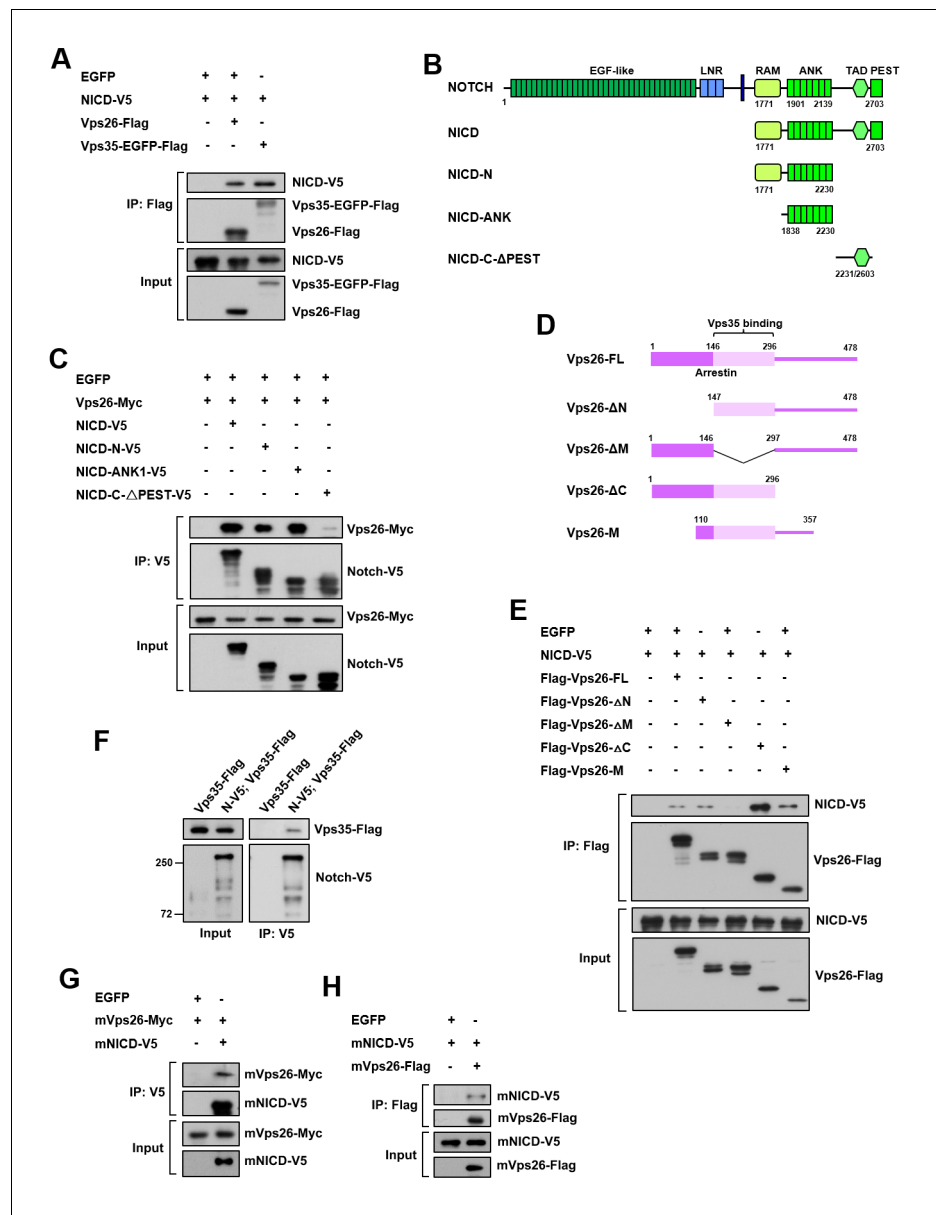


Figure 4. Retromer physically interacts with Notch. (A) Coimmunoprecipitation (CoIP) of FLAG-tagged Vps26 or Vps35 and V5-tagged Notch intracellular domain (NICD) in HEK293T cell extracts. Note that in these and subsequent panels, EGFP served as a negative control. (B) Schematic drawings of NICD protein domains and truncated constructs. (C) CoIP of full-length (FL) or truncated NICD-V5 and Vps26-Myc in HEK293T cells. (D) Schematic drawings of Vps26 protein domains and truncated constructs. (E) The reciprocal coIP of full-length (FL) or truncated FLAG-Vps26 and NICD-V5 in HEK293T cells. (F) CoIP of Vps35-FLAG and Notch-V5 (N-V5) in fly larval brain extracts. Note that Vps35-FLAG and N-V5 were specifically expressed in neuroblast lineages by *insc*-Gal4. (G,H) CoIP of Myc-tagged mouse Vps26 (mVps26-Myc) and V5-tagged mouse NICD (mNICD-V5) and the reciprocal coIP of mVps26-FLAG and mNICD-V5 in HEK293T cell extracts. DOI: <https://doi.org/10.7554/eLife.38181.015>

addition, the Delta ligand clearly colocalized with Rab7⁺ enlarged endosomes in *vps35* mutant cells (Figure 5G). Taken together, we concluded that the enlarged, aberrant endosomal vesicles with both early and late endosomal identities are the ligand-dependent activating compartments of the Notch receptor in *vps35* mutant neural progenitors.

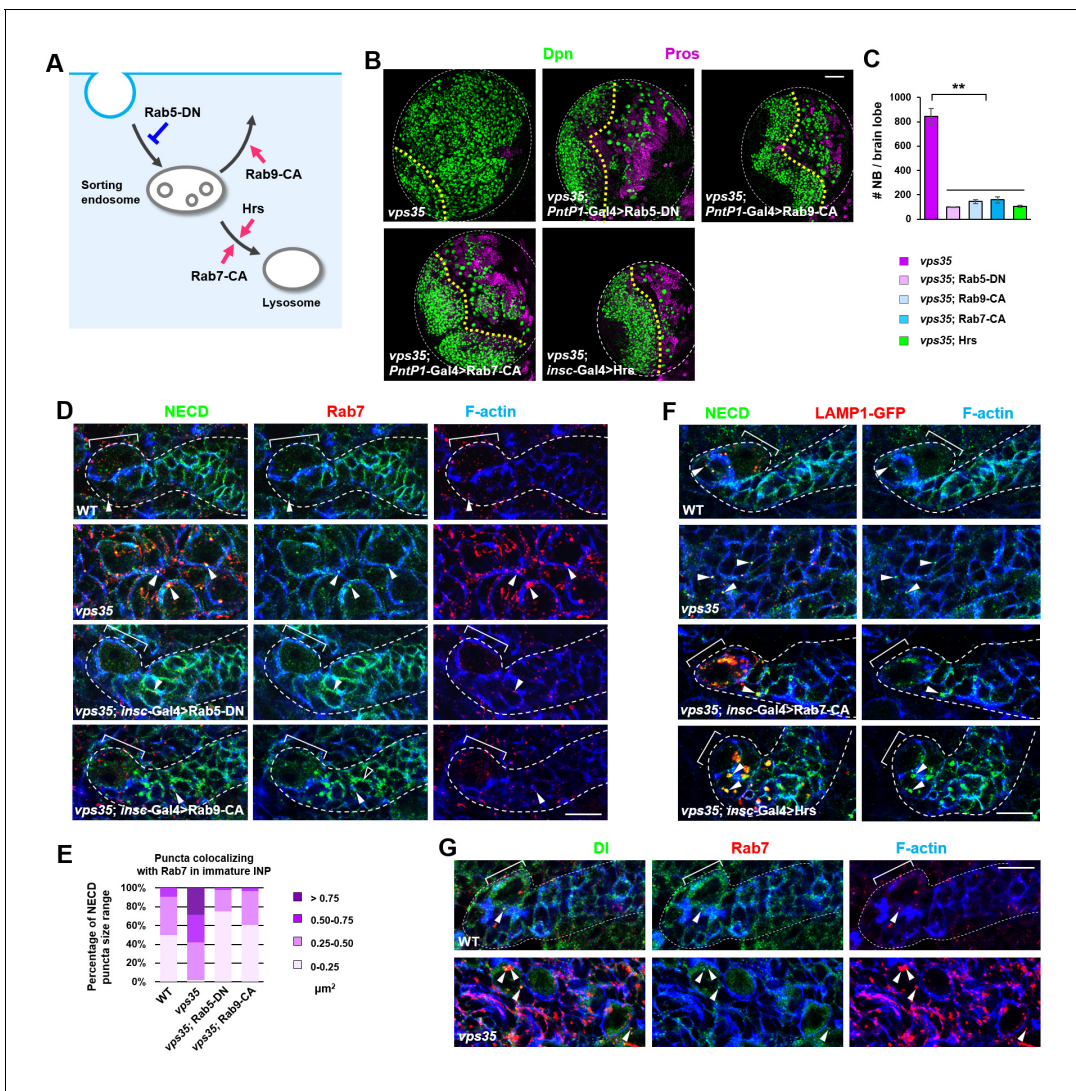


Figure 5. Retromer prevents intracellular ectopic cleavage of Notch receptors. (A) Schematic depicting a simplified endocytic pathway. Red arrow: promotion; blue flat line: inhibition. (B,C) Larval brain lobes of indicated genotypes were stained for Dpn and Pros. Quantification of total neuroblast number per brain lobe is shown in (C). ** $p < 0.001$ ($n = 10-12$). (D,E) Type II neuroblast lineages of indicated genotypes were stained for NECD, Rab7 and F-actin. NECD puncta colocalizing with Rab7 are marked with arrowheads. Quantification of the size range of Notch puncta colocalizing with Rab7⁺ endosomes is shown in (E). (F) Type II neuroblast lineages of indicated genotypes were stained for NECD, GFP and F-actin. (G) Type II neuroblast lineages of indicated genotypes were stained for Delta, Rab7 and F-actin. Scale bars, 50 μm (B) and 10 μm (D,F,G).

DOI: <https://doi.org/10.7554/eLife.38181.016>

The following source data and figure supplements are available for figure 5:

Source data 1. Input data for bar graph **Figure 5C**.

DOI: <https://doi.org/10.7554/eLife.38181.019>

Figure supplement 1. The effects of Rab5-DN, Rab9-CA, Rab7-CA or Hrs expression on Notch receptor trafficking.

DOI: <https://doi.org/10.7554/eLife.38181.017>

Figure supplement 2. Overexpression of Rab5-CA, Rab7-DN or Rab9-DN failed to inhibit the brain tumor phenotype in vps35 mutants.

DOI: <https://doi.org/10.7554/eLife.38181.018>

Retromer recycles hypo-ubiquitinated Notch receptors

Why Notch needs to be transported away from its activating compartments by retromer under physiological conditions? Previous studies indicated that the internalized Notch receptors are either sorted through the ESCRT pathway and get degraded in lysosomes or recycled back to the plasma membrane for ligand binding and activation (*Kopan, 2012*). Furthermore, ubiquitin is a crucial

sorting signal for Notch receptor trafficking. We therefore considered the intriguing possibility that a pool of hypo-ubiquitinated Notch receptors might not be sorted through ESCRT-0 but instead trapped at the limiting membrane of MVBs, where they are retrieved and transported away by retromer in a timely manner.

If this hypothesis is correct, one would expect that an elevation in the activity of the E3 ubiquitin ligase(s) that promotes Notch polyubiquitination and lysosomal degradation may reduce the pool of hypo-ubiquitinated Notch in retromer mutant neural progenitors and thereby alleviate the brain tumor phenotype. Neuroblast lineage-specific overexpression of HECT domain E3 ubiquitin ligase Itch/Su(dx) or Nedd4, known for mediating Notch receptor polyubiquitination and degradation (Cornell et al., 1999; Le Bras et al., 2011; Qiu et al., 2000; Sakata et al., 2004; Wilkin et al., 2004), showed little inhibitory effect on the supernumerary neuroblast phenotype in *vps35* mutants (Figure 6A,B), suggesting that these two E3 ligases are not fully active upon overexpression in neuroblast lineages. Since Ndfip protein (Nedd4 family interacting protein) has been reported to recruit and activate Itch/Su(dx) or Nedd4 by relieving their autoinhibition caused by intramolecular interaction (Dalton et al., 2011; Mund and Pelham, 2009), we coexpressed Ndfip in an attempt to boost the catalytic activity of Itch/Su(dx) and Nedd4. Whereas simultaneous overexpression of Nedd4 and Ndfip barely exhibited any effect on brain tumor phenotype caused by *vps35* mutation (Figure 6—figure supplement 1A–C), coexpression of Su(dx) and Ndfip indeed led to a complete rescue of the supernumerary neuroblast phenotype in *vps35* mutants (Figure 6A,B). Consistent with these observations, the high accumulation of Notch in aberrant endosomal vesicles in *vps35* mutant cells was also effectively suppressed by Su(dx) and Ndfip coexpression (Figure 6—figure supplement 1D,E).

A related and more important prediction of this hypothesis is that the activity of the E3 ubiquitin ligase(s) targeting Notch for polyubiquitination and degradation is inherently inefficient in fly neuroblast lineages and depends on retromer-mediated retrieval to avoid ectopic accumulation and processing of Notch in INPs. If this model is correct, we reason that a reduction in the activity of the E3 ubiquitin ligase(s) might tilt the balance and lead to a larger pool of hypo-ubiquitinated Notch than normal. If retromer is meanwhile not fully functional, Notch receptors may be stalled in MVBs and eventually result in progenitor-derived tumor. Indeed, we observed a strong synergistic interaction between Su(dx) and *Vps26* in mediating neuroblast self-renewal. While expression of either *vps26-RNAi* or Su(dx)-C917A, a dominant negative form of Su(dx) (Su(dx)-DN) that lacks its E3 ubiquitin ligase activity (Wang et al., 2015), by *PntP1*-Gal4, led to a mild neuroblast overproliferation phenotype (Figure 6C,D), simultaneous expression of *vps26-RNAi* and Su(dx)-DN resulted in a severe brain tumor phenotype (Figure 6C,D). More significantly, Notch receptors were highly accumulated in enlarged Rab7-positive endosomal vesicles in neural progenitors expressing both *vps26-RNAi* and Su(dx)-DN, but not in neural progenitors expressing either *vps26-RNAi* or Su(dx)-DN alone (Figure 6E,F). Immunostaining with our newly-raised Su(dx) and Ndfip antibodies (Figure 6—figure supplement 2A,B) revealed that Su(dx) mainly localized to the cell cortex, whereas Ndfip primarily distributed in intracellular vesicles (Figure 6—figure supplement 2C,D). Such largely distinct distribution pattern of Su(dx) and Ndfip in INPs might partially explain why Notch polyubiquitination and lysosomal degradation is inherently inefficient in neural progenitors.

A third prediction of this hypothesis is that ectopic processing and activation of the Notch receptor in *vps35* mutants are independent of the ESCRT pathway. Indeed, blocking the entry to the ESCRT pathway via depletion of Hrs, a key subunit of ESCRT-0, exhibited no effects on the brain tumor phenotypes in *vps35* mutants (Figure 6G,H). Taken together, these findings indicated that retromer prevents neural progenitor dedifferentiation through compensating the insufficient dampening of Notch signaling mediated by the Su(dx)/Ndfip-ESCRT-lysosomal pathway.

To further confirm this hypothesis, we assessed the cleavage status of the Notch receptor. Our model predicts that, upon retromer dysfunction, the chances for Notch to be transported back to the plasma membrane to access its E3 ubiquitin ligase(s) and obtain additional ubiquitin moieties become smaller. As a consequence, a pool of hypo-ubiquitinated Notch might accumulate and ectopically processed. In accordance, our results clearly showed that, a smear of presumably ubiquitinated NICD migrating at approximately 130 kilodaltons (kDa) and a un-ubiquitinated NICD band migrating at 100 kDa specifically accumulated in *vps35* mutant but not wild type brain extracts, indicating that these Notch fragments are hypo-ubiquitinated NICD (Figure 6I). Importantly, such increased intensity of the smear of these hypo-ubiquitinated Notch fragments in *vps35* mutants (green arrowhead) was essentially reduced back to normal upon coexpression of Su(dx) and Ndfip

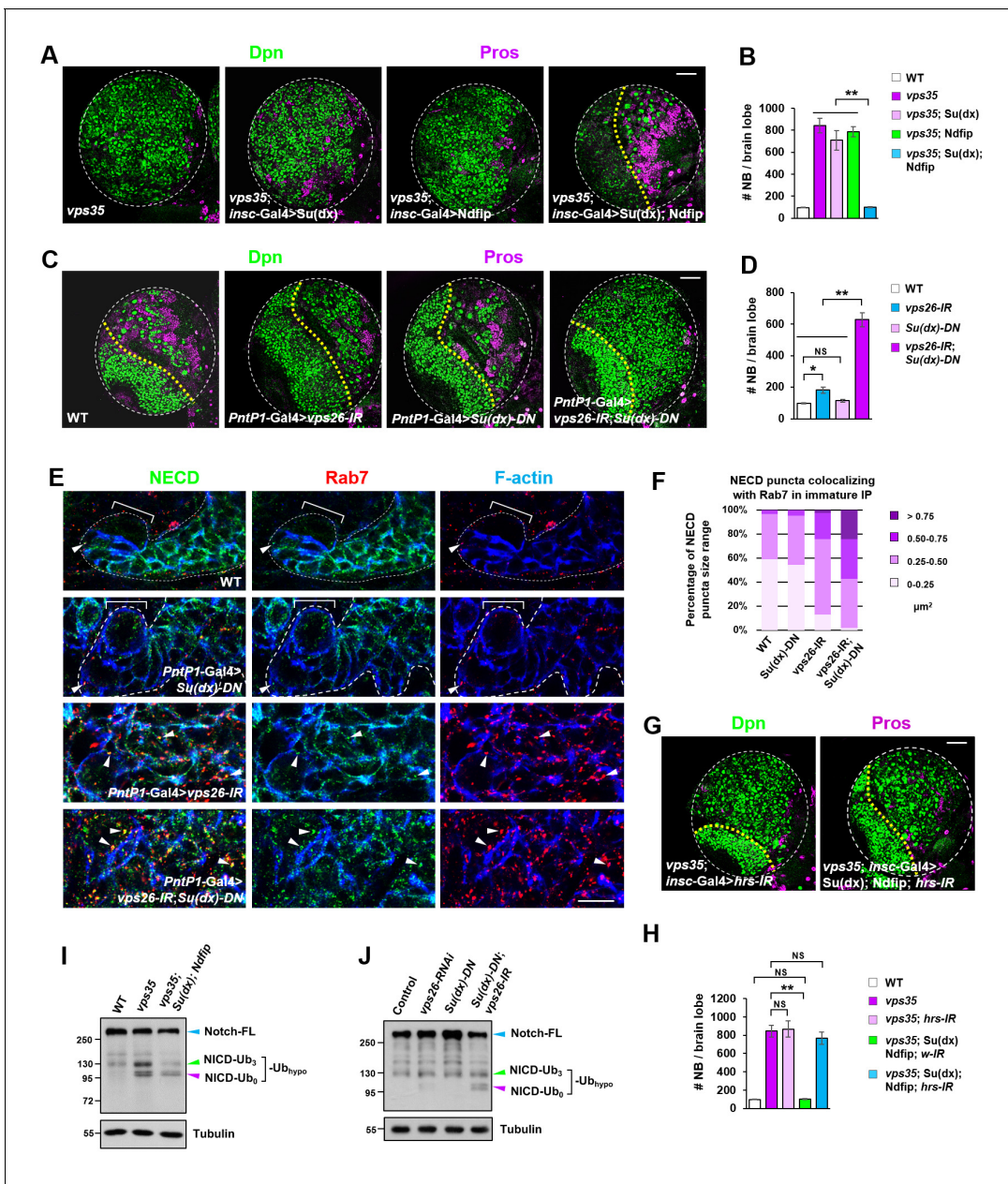


Figure 6. Retromer compensates for the inefficient Notch polyubiquitination and lysosomal degradation. (A,B) Neuroblast-specific coexpression of both *Su(dx)* and *Ndfip* but not either alone potentially inhibited brain tumor phenotype in *vps35* mutants. Quantification of total neuroblast number of indicated genotypes is shown in (B). ** $p < 0.001$ ($n = 12-15$). (C,D) Larval brain lobes of indicated genotypes were stained for Dpn and Pros. Quantification of total neuroblast number per brain lobe is shown in (D). ** $p < 0.001$; * $p < 0.01$; NS, not significant ($n = 13-15$). (E) Type II neuroblast lineages of indicated genotypes were stained for NECD, Rab7 and F-actin. NECD puncta colocalizing with Rab7 are marked with arrowheads. (F) Quantification of the size range of Notch puncta colocalizing with Rab7⁺ endosomes in immature or dedifferentiating neural progenitors of indicated genotypes. (G,H) Larval brain lobes of indicated genotypes were stained for Dpn and Pros. Quantification of total neuroblast number per brain lobe is shown in (H). ** $p < 0.001$; NS, not significant ($n = 11-15$). (I,J) Western blot analysis of larval brain extracts of indicated genotypes using anti-NICD antibody. Anti- α -tubulin blot served as a loading control. Note that hypo-ubiquitinated NICD fragments included NICD carrying approximately three ubiquitin moieties (NICD-Ub₃) and un-ubiquitinated NICD (NICD-Ub₀). Scale bars, 10 μ m (E) and 50 μ m (A,C,G).

DOI: <https://doi.org/10.7554/eLife.38181.020>

The following source data and figure supplements are available for figure 6:

Source data 1. Input data for bar graph **Figure 6B,D,H**.

DOI: <https://doi.org/10.7554/eLife.38181.025>

Figure supplement 1. Coexpression of *Su(dx)* and *Ndfip* specifically suppresses brain tumor phenotypes in *vps35* mutants.

Figure 6 continued on next page

Figure 6 continued

DOI: <https://doi.org/10.7554/eLife.38181.021>

Figure supplement 2. Distribution patterns of Su(dx) and Ndfip in type II neuroblast lineages.

DOI: <https://doi.org/10.7554/eLife.38181.022>

Figure supplement 3. Proteolytic processing of NiGFP in *Notch* mutant or *Notch*; *vps35* double mutant larval brain extracts.

DOI: <https://doi.org/10.7554/eLife.38181.023>

Figure supplement 4. Co-overexpression of Su(dx) and Ndfip caused loss of type II neuroblast lineages and brain tissue atrophy.

DOI: <https://doi.org/10.7554/eLife.38181.024>

(**Figure 6I**). We reason that coexpression of E3 ligase led to a reduction in the pool of hypo-ubiquitinated Notch and a corresponding increase in the pool of Notch harboring sufficient ubiquitin moieties, which was sorted through the ESCRT pathway and degraded in lysosomes. Indeed, blocking the cargo entry into the ESCRT pathway by Hrs downregulation potently inhibited the rescue effects of Su(dx)/Ndfip on retromer inactivation-induced brain tumor phenotype (**Figure 6G,H**). Consistently, un-ubiquitinated NICD fragments also specifically accumulated in larval brain extracts coexpressing *vps26-RNAi* and *Su(dx)-DN* but not in extracts expressing either *vps26-RNAi* or *Su(dx)-DN* alone (**Figure 6J**). Furthermore, in *N*; NiGFP background, in which a bacterial artificial chromosome (BAC) transgene expressing a GFP-tagged Notch (NiGFP) functionally replaces endogenous Notch (Couturier et al., 2012), accumulation of hypo-ubiquitinated NICD-GFP fragments was also specifically detected in *vps35* mutant but not wild type control brain extracts (**Figure 6—figure supplement 3**).

Collectively, our results supports a safeguard model whereby Notch polyubiquitination mediated by the E3 ubiquitin ligase Itch/Su(dx) is inherently inefficient within neural progenitors, relying on retromer-mediated retrograde trafficking to retrieve the pool of hypo-ubiquitinated Notch that fails to enter the ESCRT-lysosomal degradation pathway in a timely manner (**Figure 7**). Upon retromer inactivation, hypo-ubiquitinated Notch accumulates in MVBs, ectopically processed in a ligand-dependent fashion, leading to cell-autonomous activation of Notch signaling, neural progenitor dedifferentiation and tumorigenesis (**Figure 7**).

Discussion

Unidirectional Notch signaling is a widely used strategy for initiating and maintaining binary cell fates. However, the molecular mechanisms establishing the unidirectionality of Notch signaling in stem cell lineages remain unclear. Here we reveal that, while asymmetric partition of Numb leads to a biased internalization of the Notch receptor and hence asymmetric dampening of Notch signaling in neural progenitors, it meanwhile poses a high risk of non-canonical endosomal activation of Notch. We find that the retromer complex is the key protein trafficking machinery that resolves this crisis through a timely retrieval of the Notch receptor from its endosomal activation compartments. Upon retromer dysfunction, neural progenitors dedifferentiate into neural stem cell-like status and result in the formation of transplantable tumors. Therefore, retromer acts as a tumor suppressor in *Drosophila* larval brains. Importantly, mammalian Vps35 physically interacts with Notch, colocalizes with Notch in neural progenitors, and its neuroblast-lineage-specific expression fully rescues neural progenitor-derived brain tumor phenotype in *vps35* mutants. Thus, the brain tumor suppressor function of retromer is likely to be conserved in mammals. Intriguingly, downregulation of the retromer complex components has been reported in various human cancers, including glioblastoma (An et al., 2012; Bredel et al., 2005; Lee et al., 2006b). Our studies thus provide a new mechanistic link between the retromer complex and carcinogenesis.

Why the E3 ubiquitin ligase system promoting Notch receptor polyubiquitination and degradation is inherently inefficient in neuroblast lineages? We speculate that Notch is probably not the only substrate of Su(dx) and Ndfip in neuroblasts or neural progenitors. Therefore, high levels and/or activity of this E3 ubiquitin ligase system above certain threshold may potentially cause imbalanced homeostasis of its critical substrates and hence perturbed neuroblast lineages. Indeed, co-overexpression of Su(dx) and Ndfip led to drastically reduced number of neuroblast lineages and severe tissue atrophy (**Figure 6—figure supplement 4**). In this case, a relatively general yet inefficient ubiquitination-degradation system coupled with a highly efficient and selective cargo retrieving

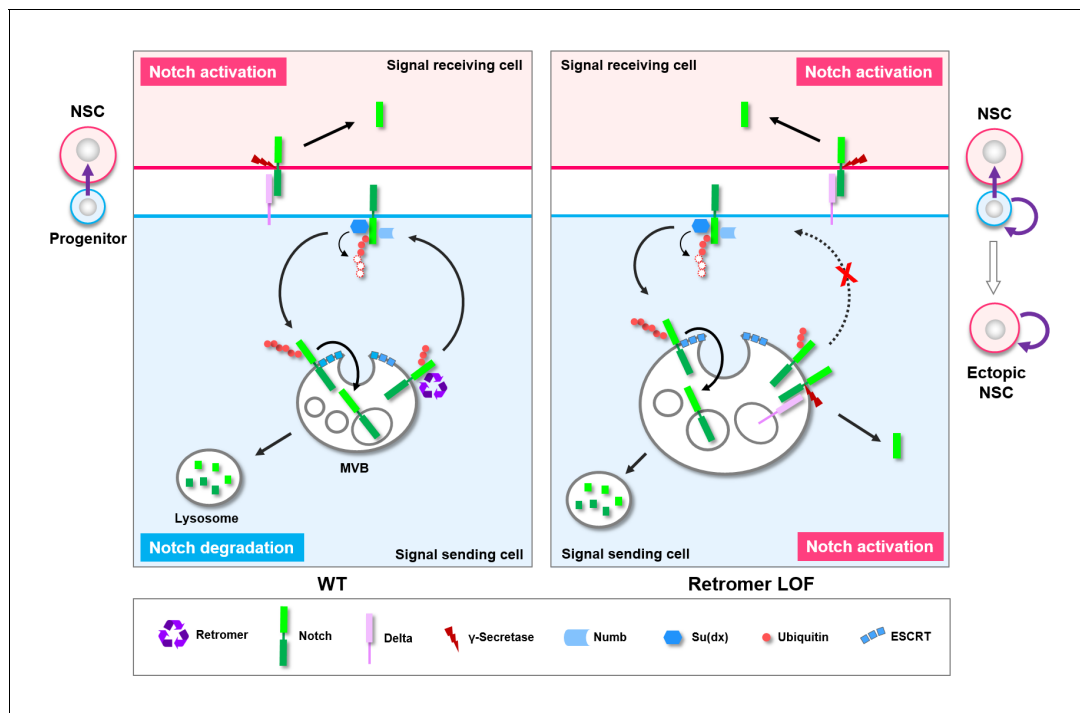


Figure 7. Working model. A graphic model depicting a safeguard mechanism whereby retromer ensures unidirectional Notch signaling (purple arrow) from neural progenitor (light blue) to neural stem cell (NSC; pink) by preventing cell-autonomous ectopic Notch signaling activation in neural progenitors. Retromer (purple) normally interacts with Notch (green) and retrieves the pool of hypoubiquitinated Notch evading the ESCRT (cyan)-lysosomal degradation pathway and sends it back to the cell surface (left panel). Upon retromer dysfunction, hypoubiquitinated Notch is accumulate in MVBs and aberrantly cleaved by γ -secretase (brown) in a ligand (light purple)-dependent manner, causing neural progenitor-originated tumorigenesis (right panel).

DOI: <https://doi.org/10.7554/eLife.38181.026>

system provides a customized regulation of the Notch receptor, ensuring sufficient dampening of Notch signaling in neural progenitors without devastating side effects.

Intriguingly, previous studies posited that retromer dysfunction causes increased levels of APP (β -amyloid precursor protein) to reside in the endosomes for longer duration than normal, resulting in accelerated processing of APP into amyloid- β , a neurotoxic fragment implicated AD pathogenesis (*Small and Gandy, 2006; Small and Petsko, 2015*). Furthermore, retromer maintains the integrity of photoreceptors by avoiding persistent accumulation of rhodopsin in endolysosomal compartments that stresses photoreceptors and causes their degeneration (*Wang et al., 2014*). Taken together with our study here, these findings indicate that retromer serves as bomb squad to retrieve and disarm harmful or toxic protein fragments from endosomes in a timely manner and thereby safeguard the integrity and fitness of the neuronal lineages.

How is the Notch receptor ectopically activated in retromer mutants? We favor the idea that Notch is activated in MVBs in a ligand-dependent, cell-autonomous manner, distinct from the majority of non-canonical Notch activation mechanisms. Most of the endosomal Notch activation events identified before, including ectopic Notch signaling activation in ESCRT mutants, BLOS2 mutants, or Rme8 and Vps26 double knockdown background, as well as Hif- α -dependent activation of Notch signaling implicated in crystal cell maintenance and survival, are all ligand-independent (*Baron, 2012; Childress et al., 2006; Gallagher and Knoblich, 2006; Giebel and Wodarz, 2006; Gomez-Lamarca et al., 2015; Hori et al., 2011; Jaekel and Klein, 2006; Mukherjee et al., 2011; Palmer and Deng, 2015; Schneider et al., 2013; Thompson et al., 2005; Vaccari and Bilder, 2005; Vaccari et al., 2009; Wilkin et al., 2008; Zhou et al., 2016*). It has been proposed that the proteases within the acidifying environment of MVB lumen are sufficient to remove the extracellular domain of Notch, leading to the S3 cleavage of Notch at the limiting membrane (*Palmer and Deng, 2015; Wilkin et al., 2008*). Strongly supporting this notion, blocking the entry of Notch into the

ESCRT pathway but not ligand inactivation potently inhibited ectopic Notch activation induced by ESCRT mutations (*Childress et al., 2006; Gallagher and Knoblich, 2006; Jaekel and Klein, 2006*). In sharp contrast to these previously-revealed mechanisms, attenuating ligand activity but not preventing Notch from entering the ESCRT pathway effectively rescues Notch overactivation phenotype caused by retromer dysfunction (*Figures 3D,E and 6G,H*). Then how Notch signaling is ectopically activated in a ligand-dependent manner in retromer mutants? We speculate that, upon retromer dysfunction, both Notch and Delta are entrapped in MVBs, where Notch and Delta are presented by limiting membrane and intravesicular membrane respectively and result in ligand-dependent Notch processing and activation, resembling the scenario presented for ligand-dependent Notch signaling activation in Sara endosome (*Coumaillau et al., 2009; Kressmann et al., 2015*). The detailed regulatory mechanisms underlying Notch overactivation in retromer mutants warrants future investigation.

The ability of *vps35* mutant neoplastic neuroblasts to metastasize upon transplantation is intriguing (*Figure 1J,K*). Metastasis of brain tumor cells derived from neuroblast lineages has never been observed in the developing fly larval brains, likely because the limited time window of fly larval development precludes tumor progression and metastasis. Transplantation assay (*Rossi and Gonzalez, 2015*), however, provides the ectopic microenvironment and allows cancer progression in a much longer time scale (months, or even years upon retransplantation). Importantly, mutations that caused metastasis of fly brain tumor cells upon transplantation have also been implicated in various human cancers (*Caussinus and Gonzalez, 2005; Eroglu et al., 2014; Froidi et al., 2015; Knoblich, 2010; Landskron et al., 2018; Liu et al., 2017; Narbonne-Reveau et al., 2016*). Future studies on the transcriptional profiling of the distal metastatic colonies and stepwise characterization of this long-range metastatic process promise to provide us with fresh mechanistic insights into the enormously complex process of cancer metastasis.

Materials and methods

Key resources table

Reagent type (species) or resource	Designation	Source or reference	Identifiers	Additional information
Genetic reagent (<i>D. melanogaster</i>)	<i>insc</i> -Gal4	(<i>Luo et al., 1994</i>)	N/A	
Genetic reagent (<i>D. melanogaster</i>)	<i>PntP1</i> -Gal4	(<i>Zhu et al., 2011</i>)	N/A	
Genetic reagent (<i>D. melanogaster</i>)	<i>ase</i> -Gal4	(<i>Zhu et al., 2006</i>)	N/A	
Genetic reagent (<i>D. melanogaster</i>)	<i>erm</i> -Gal4 (II)	(<i>Xiao et al., 2012</i>)	N/A	
Genetic reagent (<i>D. melanogaster</i>)	<i>erm</i> -Gal4 (III)	(<i>Pfeiffer et al., 2008; Weng et al., 2010</i>)	N/A	
Genetic reagent (<i>D. melanogaster</i>)	UAS- <i>vps26</i> -RNAi	Bloomington Drosophila Stock Center	RRID: BDSC_38937	
Genetic reagent (<i>D. melanogaster</i>)	UAS- <i>Notch</i> -RNAi	Vienna Drosophila RNAi Center	RRID: VDRC_27229	
Genetic reagent (<i>D. melanogaster</i>)	UAS- <i>Delta</i> -RNAi	Bloomington Drosophila Stock Center	RRID: BDSC_34322	
Genetic reagent (<i>D. melanogaster</i>)	UAS- <i>wg</i> -RNAi	Bloomington Drosophila Stock Center	RRID: BDSC_32994	
Genetic reagent (<i>D. melanogaster</i>)	UAS- <i>med</i> -RNAi	Bloomington Drosophila Stock Center	RRID: BDSC_52214	
Genetic reagent (<i>D. melanogaster</i>)	UAS- <i>Hrs</i> -RNAi	Bloomington Drosophila Stock Center	RRID: BDSC_34086 ; BDSC_33900	
Genetic reagent (<i>D. melanogaster</i>)	UAS- <i>white</i> -RNAi	Bloomington Drosophila Stock Center	RRID: BDSC_33644	

Continued on next page

Continued

Reagent type (species) or resource	Designation	Source or reference	Identifiers	Additional information
Genetic reagent (<i>D. melanogaster</i>)	UAS-Vps26-Myc	This paper	N/A	
Genetic reagent (<i>D. melanogaster</i>)	UAS-Vps35-FLAG	This paper	N/A	
Genetic reagent (<i>D. melanogaster</i>)	UAS-hVps35-FLAG	This paper	N/A	
Genetic reagent (<i>D. melanogaster</i>)	UAS-HA-Rab9-CA	This paper	N/A	
Genetic reagent (<i>D. melanogaster</i>)	UAS-Myc-Su(dx)	This paper	N/A	
Genetic reagent (<i>D. melanogaster</i>)	UAS-Myc-Su(dx)-C917A	This paper	N/A	
Genetic reagent (<i>D. melanogaster</i>)	UAS-Myc-Nedd4	This paper	N/A	
Genetic reagent (<i>D. melanogaster</i>)	UAS-FLAG-Ndfip	This paper	N/A	
Genetic reagent (<i>D. melanogaster</i>)	UAS-Su(dx)	Bloomington Drosophila Stock Center	RRID: BDSC_51664	
Genetic reagent (<i>D. melanogaster</i>)	UAS-Hrs	(Lloyd et al., 2002)	N/A	
Genetic reagent (<i>D. melanogaster</i>)	UAS-Spdo-GFP	(Song and Lu, 2012)	N/A	
Genetic reagent (<i>D. melanogaster</i>)	UAS-DI-DN	Bloomington Drosophila Stock Center	RRID: BDSC_26698	
Genetic reagent (<i>D. melanogaster</i>)	UAS-Psn-DN	Bloomington Drosophila Stock Center	RRID: BDSC_8323	
Genetic reagent (<i>D. melanogaster</i>)	UAS-Kuz-DN	Bloomington Drosophila Stock Center	RRID: BDSC_6578	
Genetic reagent (<i>D. melanogaster</i>)	UAS-EGFR-DN	Bloomington Drosophila Stock Center	RRID: BDSC_5364	
Genetic reagent (<i>D. melanogaster</i>)	UAS-ptc-DN	Bloomington Drosophila Stock Center	RRID: BDSC_31928	
Genetic reagent (<i>D. melanogaster</i>)	UAS-GFP-LAMP1	Bloomington Drosophila Stock Center	RRID: BDSC_42714	
Genetic reagent (<i>D. melanogaster</i>)	UAS-mito-GFP	Bloomington Drosophila Stock Center	RRID: BDSC_8442	
Genetic reagent (<i>D. melanogaster</i>)	sqh-EYFP-Golgi	Bloomington Drosophila Stock Center	RRID: BDSC_7193	
Genetic reagent (<i>D. melanogaster</i>)	UAS-YFP-Rab5-WT	Bloomington Drosophila Stock Center	RRID: BDSC_24616	
Genetic reagent (<i>D. melanogaster</i>)	UAS-YFP-Rab5-CA	Bloomington Drosophila Stock Center	RRID: BDSC_9773	
Genetic reagent (<i>D. melanogaster</i>)	UAS-Rab5-DN	Bloomington Drosophila Stock Center	RRID: BDSC_42704	
Genetic reagent (<i>D. melanogaster</i>)	UASp-YFP-Rab7-DN	Bloomington Drosophila Stock Center	RRID: BDSC_9778	
Genetic reagent (<i>D. melanogaster</i>)	UAS-Rab7-CA	Bloomington Drosophila Stock Center	RRID: BDSC_42707	
Genetic reagent (<i>D. melanogaster</i>)	UASp-YFP-Rab9-WT	Bloomington Drosophila Stock Center	RRID: BDSC_9784	
Genetic reagent (<i>D. melanogaster</i>)	UASp-YFP-Rab9-CA	Bloomington Drosophila Stock Center	RRID: BDSC_9785	

Continued on next page

Continued

Reagent type (species) or resource	Designation	Source or reference	Identifiers	Additional information
Genetic reagent (<i>D. melanogaster</i>)	UASp-YFP-Rab9-DN	Bloomington Drosophila Stock Center	RRID: BDSC_23642	
Genetic reagent (<i>D. melanogaster</i>)	UAS-YFP-Rab11-DN	Bloomington Drosophila Stock Center	RRID: BDSC_9792	
Genetic reagent (<i>D. melanogaster</i>)	<i>vps35^{E42}</i>	Gift from Xinhua Lin (Belenkaya et al., 2008)	N/A	
Genetic reagent (<i>D. melanogaster</i>)	<i>vps35¹</i>	Gift from Xinhua Lin (Belenkaya et al., 2008)	N/A	
Genetic reagent (<i>D. melanogaster</i>)	<i>N^{55e11}</i> ; NiGFP	(Couturier et al., 2012)	N/A	
Genetic reagent (<i>D. melanogaster</i>)	UAS-FLP, Ubi-p63E-FRT-nlsGFP	Bloomington Drosophila Stock Center	RRID: BDSC_28282	
Antibody	Mouse anti-Notch ^{ECD} (C458.2H)	Developmental Studies Hybridoma Bank	RRID: AB_528408	IHC (1:80)
Antibody	Mouse anti-Pros (MR1A)	Developmental Studies Hybridoma Bank	RRID: AB_528440	IHC (1:100)
Antibody	Rat anti-Mira	Abcam	Cat#Ab197788	IHC (1:100)
Antibody	Rabbit anti-Dpn	Gift from Y.N. Jan	N/A	IHC (1:1000)
Antibody	Guinea pig anti-Numb	Gift from J. Skeath (O'Connor-Giles and Skeath, 2003)	N/A	IHC (1:1000)
Antibody	Mouse anti-β-galactosidase (40-1a)	Developmental Studies Hybridoma Bank	RRID: AB_2314509	IHC (1:100)
Antibody	Guinea pig anti-Ase	Gift from Y.N. Jan	N/A	IHC (1:400)
Antibody	Rabbit anti-aPKC ζ C20	Santa Cruz Biotechnologies	RRID: AB_2168668	IHC (1:1000)
Antibody	Rabbit anti-Rab7	Gift from A. Nakamura (Tanaka and Nakamura, 2008)	N/A	IHC (1:2000)
Antibody	Mouse anti-Wg (4D4)	Developmental Studies Hybridoma Bank	RRID: AB_528512	IHC (1:100)
Antibody	Mouse anti-Ptc (Apa 1)	Developmental Studies Hybridoma Bank	RRID: AB_528441	IHC (1:100)
Antibody	Rabbit anti-Myc (71D10)	Cell Signaling Technology	RRID: AB_10693332	WB (1:2000)
Antibody	Rabbit anti-FLAG	Sigma-Aldrich	RRID: AB_439687	IHC (1:1000)
Antibody	Rabbit anti-V5	Sigma-Aldrich	RRID: AB_261889	WB (1:1000)
Antibody	Mouse anti-c-Myc	CW Biotech	Cat#cw0299M	WB (1:2000)
Antibody	Mouse anti-Delta ^{ECD} (C594.9B)	Developmental Studies Hybridoma Bank	RRID: AB_528194	IHC (1:200)
Antibody	Mouse anti-Notch ^{ICD} (C17.9C6)	Developmental Studies Hybridoma Bank	RRID: AB_528410	WB (1:1000)
Antibody	Rabbit anti-Vps26	This paper	N/A	IHC (1:200)
Antibody	Rabbit anti-Su(dx)	This paper	N/A	IHC (1:200)
Antibody	Rabbit anti-Ndfip	This paper	N/A	IHC (1:100)
Antibody	Anti-V5 affinity gels	Sigma-Aldrich	RRID: AB_10062721	15 μl gel per colP reaction
Antibody	Anti-FLAG M2 affinity gels	Sigma-Aldrich	RRID: AB_10063035	15 μl gel per colP reaction
Software, algorithm	ImageJ	NIH	N/A	
Software, algorithm	Photoshop CS5	Adobe	N/A	
Software, algorithm	The Leica Application Suite 2.6.3	Leica	N/A	
Cell line (Human)	HEK293T	ATCC	RRID: CRL-3216	
Recombinant DNA reagent	pcDNA3.1	Invitrogen	Cat#: V79020	

Continued on next page

Continued

Reagent type (species) or resource	Designation	Source or reference	Identifiers	Additional information
Recombinant DNA reagent	vps26 (<i>Drosophila</i> cDNA)	BDGP	LD29140	
Recombinant DNA reagent	vps35-RB (<i>Drosophila</i> cDNA)	BDGP	SD03023	
Recombinant DNA reagent	nedd4-RK (<i>Drosophila</i> cDNA)	BDGP	SD04682	
Recombinant DNA reagent	vps35 (<i>human</i> cDNA)	Human ORFeome	Internal ID: 7965 Genbank Accession: CV029249	
Recombinant DNA reagent	vps26A (<i>human</i> cDNA)	Addgene	Cat#17636	
Recombinant DNA reagent	NICD1 (<i>mouse</i> cDNA)	Addgene	Cat#20183	

Fly genetics

Fly culture and crosses were performed according to standard procedures. *Drosophila* stocks used in this study include: vps35^{E42} (Belenkaya et al., 2008) (a gift from Dr. Xinhua Lin); vps35¹ (Belenkaya et al., 2008); vps26^{G2008} (BL26623); UAS-Vps35-FLAG (this study); UAS-Vps26-Myc (RR: RNAi resistant form; this study); UAS-vps26-RNAi (BL38937); UAS-Notch-RNAi (VDRC27229); UAS-DI-DN (BL26698); UAS-DI-RNAi (BL34322); UAS-Psn-DN (BL8323); UAS-Kuz-DN (BL6578); UAS-Rab5-DN (BL42704); UAS-Rab7-CA (BL42707); UAS-Hrs (Lloyd et al., 2002); UAS-GFP-LAMP1 (BL42714); UAS-mito-GFP (BL8442); UASp-YFP-Rab9-WT (BL9784); UASp-YFP-Rab9-CA (BL9785); UAS-Su(dx) (BL51664); UAS-Myc-Su(dx) (this study); UAS-FLAG-Ndfip (this study); UAS-Myc-Su(dx)-C917A (this study); UAS-Myc-Nedd4 (this study); *insc*-Gal4 (Luo et al., 1994); *PntP1*-Gal4 (Zhu et al., 2011); *ase*-Gal4 (Zhu et al., 2006); *erm*-Gal4 (II) (Xiao et al., 2012); *erm*-Gal4 (III) (Pfeiffer et al., 2008; Weng et al., 2010); E(spl)my-GFP (Almeida and Bray, 2005; Monastirioti et al., 2010); UAS-Spdo-GFP (Song and Lu, 2012); UAS-wg-RNAi (BL32994); UAS-EGFR-DN (BL5364); UAS-med-RNAi (BL52214); UAS-ptc-DN (BL31928); UAS-Hrs-RNAi (BL34086, BL33900); N^{5se11}; NiGFP (Couturier et al., 2012) and UAS-FLP, Ubi-p63E-FRT > stop > FRT-nlsGFP (BL28282) (Evans et al., 2009).

All larval brains phenotypes were analyzed at late third instar larval stage. Note that, compared to wild type control, the development of vps35^{E42} mutant larvae was delayed. Experiments with no special notification were carried out as follows: Eggs were collected for 4–6 hr at 25°C and kept at 25°C until dissection at late third instar larval stage.

The experimental conditions shown in Figures 1D, F, 3D, 5B, D, F, 6C, E and I are as follows: Eggs were collected for 4–6 hr at 22°C, kept at 22°C for 24 hr (Figures 1D, F, 3D, 5B, 6C and E) or 48 hr (Figures 5D, F and 6I) after hatching and shifted to 29°C until dissection at late third instar larval stage. The experimental conditions shown in 3C is as follows: Eggs were collected for 4–6 hr at 25°C, kept at 18°C for 8 days, then shifted to 29°C for 40 hr before dissection. The experimental conditions shown in Figure 1—figure supplement 2 and Figure 6—figure supplement 4 are as follows: Eggs were collected for 4–6 hr at 22°C. Larvae were raised at 29°C immediately after hatching until dissection at late third instar larval stage.

Molecular biology

Full-length cDNA clones for vps35, vps26 (LD29140), and nedd4 were obtained from *Drosophila* Genomics Resource Center (DGRC). For ndfip and su(dx) cDNAs, their respective coding exons were cloned by genomic DNA PCR from w¹¹¹⁸ flies and UAS-Su(dx) transgenic flies respectively, assembled together by the Gibson Assembly method and fully sequenced. FLAG-Ndfip, Myc-Nedd4 and Myc-Su(dx)-WT were constructed by adding a FLAG tag (DYKDDDDK) or a Myc tag (EQKLISEEDL) respectively to the N-terminus. Vps35-FLAG and Vps26-Myc were constructed by adding a FLAG tag or a Myc tag respectively to the C-terminus. Note that shmiRNA-resistant sequence was introduced into Vps26 before it was cloned into the pUAST vector. A missense mutation (C917A) was introduced into Su(dx) to generate a ligase-inactivated form. NICD-V5 was generated as described

before (Liu *et al.*, 2017). All transgenic plasmids were verified by DNA sequencing before germline transformation.

For coimmunoprecipitation experiments, Vps26-FLAG and Vps26-Myc were cloned into pcDNA3.1 vector respectively (Invitrogen). Vps26 truncated forms Vps26-ΔN (aa 147–478), Vps26-ΔM (aa 1–146 and aa 297–478), Vps26-ΔC (aa 1–296) and Vps26-M (aa 110–357) were cloned with a N-terminal FLAG tag into pcDNA3.1 vector respectively. Mouse NICD cDNA was obtained from Addgene, while mouse vps26 cDNA were generated by introducing I16V, V17A, E217D to human vps26 cDNA (Addgene). NICD-V5 construct was generated as described before (Liu *et al.*, 2017), except that aa 1767–1770, 1832–1835, 2202–2205 and 2222–2225 were deleted to remove its nuclear localization sequence. NICD truncated versions NICD-N (aa 1771–2230) and NICD-ANK (aa 1838–2230) were cloned into the vector pcDNA3.1 with V5 tag added to C-terminus, and NICD-C-ΔPEST (aa 2231–2603) with a V5 tag inserted between aa 2571 and 2572. To generate mouse NICD-ΔNLS-V5, aa 1749–1752, 1771–1774, 1811–1814, 2146–2149 and 2167–2170 were deleted from mouse NICD (aa 1744–2531 of mouse Notch1 protein) and a V5 tag was inserted between aa 2396 and 2397, before cloned into pcDNA3.1 vector. mVps26-FLAG and mVps26-Myc were cloned into the pCMV vector respectively.

MARCM clonal analysis

Neuroblast MARCM clones were generated as previously described (Song and Lu, 2011). Briefly, newly hatched larvae were heat-shocked at 37°C for 90 min and further aged at 25°C for indicated time before dissection. FRTG13, vps35¹ was used for neuroblast MARCM clonal analysis, as shown in Figure 11 and Figure 1—figure supplement 2, with FRTG13 alone serving as a negative control.

Immunohistochemistry

For larval brain immunostaining, larvae were dissected in Schneider's Insect Medium (Sigma-Aldrich) and proceeded as previously described (Liu *et al.*, 2017; Song and Lu, 2011). Briefly, larval brains were fixed with 4% paraformaldehyde in PEM buffer (100 mM PIPES at pH 6.9, 1 mM EGTA, 1 mM MgCl₂) for 22 min at room temperature. Brains were washed several times with PBST buffer (1 × PBS plus 0.1% Triton X-100) and were incubated with appropriate primary antibody overnight at 4°C or for 2 hr at room temperature, labeled with secondary antibodies according to standard procedures, and mounted in Vectashield (Vector Laboratories). For anti-Delta staining, larval brains were fixed with 4% paraformaldehyde/PEM buffer for 20 min at room temperature, blocked in 3% BSA/PBST for 20 min at room temperature, before being incubated with mouse anti-Delta (1:200) in 0.5% BSA/PBST for 12 hr at 4°C. After washing with PBST buffer, brains were incubated with goat anti-mouse secondary antibody (1:100) in 0.5% BSA/PBST for 2 hr at room temperature before being mounted in Vectashield.

Antibodies generated in this study were rabbit anti-Vps26 antibody [GST fusion of aa 320–478, affinity purified (Abclonal Biotech.), used at 1:200], rabbit anti-Su(dx) [GST fusion of aa 350–500, affinity-purified (Abclonal Biotech.), used at 1:200] and rabbit anti-Ndfip [GST fusion of aa 2–165, affinity-purified (Abclonal Biotech.), used at 1:100]. To eliminate any non-specific binding, all antibodies were preabsorbed before being used in immunostaining experiments. Images were obtained on a Leica TCS SP8 AOBS confocal microscope and were processed with LAS AF (Leica) and Adobe Photoshop CS5.

Other primary antibodies used for immunohistochemistry were chicken anti-GFP (1:2000, Abcam), mouse anti-Pros (1:100, Developmental Studies Hybridoma Bank [DSHB]), mouse anti-N^{ECD} C458.2H (1:80, DSHB), rat anti-Miranda (1:100; Abcam), rabbit anti-Dpn (1:1000, Y.N. Jan), rabbit anti-Rab7 (1:2000, a generous gift from A. Nakamura) (Tanaka and Nakamura, 2008); guinea pig anti-Numb (1:1000, a generous gift from J. Skeath) (O'Connor-Giles and Skeath, 2003), mouse anti-β-galactosidase (1:100, DSHB), guinea pig anti-Ase (1:400, Y.N. Jan), rabbit anti-aPKC ζ C20 (1:1000, Santa Cruz Biotechnologies) and mouse anti-DI^{ECD} C594.9B (1:200, DSHB). The outline of individual, dispersed neuroblast lineages was determined by the staining pattern of general cell cortex marker F-actin or CD8-GFP/CD8-RFP and marked by white dashed line.

Cell line and transfection

Human embryonic kidney HEK293T cells (ATCC, RRID: [CRL-3216](#); obtained from Dr. Hong Wu's laboratory, Peking University, and authenticated by ATCC) were maintained in DMEM medium (Invitrogen) supplemented with 10% FBS at 37°C and 5% CO₂. DNA transfection was performed using a standard polyethylenimine (PEI) protocol. The cell line has been tested for and confirmed to be negative for mycoplasma contamination, using short tandem repeat (STR) profiling technique.

Coimmunoprecipitation

Coimmunoprecipitation (CoIP) assays in HEK 293 T cell extracts were performed as previously described ([Liu et al., 2017](#); [Song and Lu, 2012](#)). Briefly, 48 hr after transfection, HEK 293 T cells were harvested, washed and resuspended in lysis buffer [50 mM Tris-HCl (pH 8.0); 120 mM NaCl; 5 mM EDTA; 1% NP-40; 10% glycerol; protease inhibitor cocktail (Sigma-Aldrich); 2 mM Na₃VO₄] and kept on ice for 20 min. Cell extracts were sonicated with Bioruptor Plus (Biosense) at 4°C. The cell extracts were clarified by centrifugation, and proteins immobilized by binding to anti-FLAG M2 or anti-V5 (Sigma-Aldrich) affinity gel for 4 hr or overnight at 4°C. Beads were washed and proteins recovered directly in SDS-PAGE sample buffer. Rabbit anti-FLAG (Sigma-Aldrich), rabbit anti-V5 (Sigma-Aldrich) or mouse anti-c-Myc (CWBI) were used for Western blot analysis.

For in vivo coIP, larval brains coexpressing UAS-Vps35-FLAG and UAS-Notch-V5 by *insc-Gal4* were used as experimental group, whereas larval brains expressing UAS-Vps35-FLAG alone by *insc-Gal4* served as control. Approximately 350 late third instar larval brains of each genotype were dissected and collected in ice-cold 1xPBS solution. Protein samples were prepared by grinding brains in lysis buffer [50 mM Tris-HCl, 120 mM NaCl, 5 mM EDTA, 10% glycerol, 1% NP-40, protease inhibitor cocktail (Sigma-Aldrich)] with a plastic pestle. Immunoprecipitation was carried out with anti-V5 affinity gels (Sigma-Aldrich).

Transplantation assay

GFP⁺ larval brain pieces were transplanted into the abdomen of young female adult host flies as previously described ([Caussinus and Gonzalez, 2005](#); [Liu et al., 2017](#)). After transplantation, host flies were transferred to fresh food every day and were observed under a fluorescent scope every two days to analyze tumor formation and metastasis.

Transmission electron microscopy (TEM)

Drosophila late third instar larval brains were dissected in PBS buffer, and immediately transferred into Fixation buffer I (2% paraformaldehyde/2.5% glutaraldehyde in 0.1 M phosphate buffer, pH 7.4) for 2 hr at room temperature, and then overnight at 4°C. The samples were then fixed in the Fixation buffer II (1% tannic acid/2.5% glutaraldehyde in 0.1 M phosphate buffer, pH 7.4) for 2 hr at room temperature. After rinsing several times in phosphate buffer, the brain samples were post-fixed in 2% OsO₄ with 1.5% Potassium Ferrocyanide for 1 hr at room temperature and stained with 2% aqueous uranyl acetate overnight at 4°C. Following several washes in distilled water, samples were dehydrated through a graded alcohol series and subsequently embedded in Spurr's resin (SPI supplies, PA, USA). Ultra-thin sections (70 nm) were cut with a diamond knife using an ultramicrotome (UC7, Leica Microsystem) and mounted on copper grids with a single slot. Sections were stained with uranyl acetate and lead citrate, and observed under a FEI Tecnai G2 Spirit transmission electron microscope at 120 kV.

Acknowledgements

We are grateful to Drs. Hugo Bellen, Sarah J Bray, Chris Q Doe, Yuh-Nung Jan, Renjie Jiao, Tzumin Lee, Xinhua Lin, Bingwei Lu, Liqun Luo, Fumio Matsuzaki, Akira Nakamura, Yi Rao, Gerald M Rubin, François Schweisguth, James B Skeath, Esther M Verheyen, Hong Wu, University of Iowa DSHB, VDRC, Bloomington *Drosophila* Stock Center, and the TRiP at Harvard Medical School and Tsinghua University for fly stocks and reagents. We thank Dr. Ying-Chun Hu, Yun-Chao Xie and Hong-Mei Zhang for their professional technical assistance in TEM sample preparation and image analysis at the Core Facilities of School of Life Sciences, Peking University. We thank Dr. Francois Guillemot for helpful discussion, Dr. Bingwei Lu for supporting this project while it was in its infancy, Ms. Qiuju Zhu

for technical assistance, and members of the Song lab for discussions and help. This work was supported by the National Natural Science Foundation of China [31471372 and 31771629 to YS], the Peking-Tsinghua Center for Life Sciences (to YS) and the Ministry of Education Key Laboratory of Cell Proliferation and Differentiation (to YS).

Additional information

Funding

Funder	Grant reference number	Author
National Natural Science Foundation of China	31471372	Yan Song
Peking-Tsinghua Center for Life Sciences		Yan Song
Ministry of Education Key Laboratory of Cell Proliferation and Differentiation		Yan Song
National Natural Science Foundation of China	31771629	Yan Song

The funders had no role in study design, data collection and interpretation, or the decision to submit the work for publication.

Author contributions

Bo Li, Conceptualization, Data curation, Formal analysis, Supervision, Funding acquisition, Methodology, Writing—original draft, Writing—review and editing; Chouin Wong, Conceptualization, Data curation, Formal analysis, Investigation, Methodology, Writing—review and editing; Shihong Max Gao, Conceptualization, Data curation, Formal analysis, Methodology, Writing—review and editing; Rulan Zhang, Data curation, Formal analysis, Investigation, Methodology, Writing—review and editing; Rongbo Sun, Resources, Formal analysis, Investigation, Methodology, Writing—review and editing; Yulong Li, Resources, Formal analysis, Supervision, Investigation, Methodology, Writing—review and editing; Yan Song, Conceptualization, Data curation, Formal analysis, Supervision, Funding acquisition, Investigation, Methodology, Writing—original draft, Writing—review and editing

Author ORCIDs

Yan Song  <http://orcid.org/0000-0002-1413-6123>

Decision letter and Author response

Decision letter <https://doi.org/10.7554/eLife.38181.030>

Author response <https://doi.org/10.7554/eLife.38181.031>

Additional files

Supplementary files

- Transparent reporting form

DOI: <https://doi.org/10.7554/eLife.38181.027>

Data availability

All data generated or analysed during this study are included in the manuscript and supporting files.

References

Almeida MS, Bray SJ. 2005. Regulation of post-embryonic neuroblasts by *Drosophila* grainyhead. *Mechanisms of Development* **122**:1282–1293. DOI: <https://doi.org/10.1016/j.mod.2005.08.004>, PMID: 16275038

- An CH, Kim YR, Kim HS, Kim SS, Yoo NJ, Lee SH. 2012. Frameshift mutations of vacuolar protein sorting genes in gastric and colorectal cancers with microsatellite instability. *Human Pathology* **43**:40–47. DOI: <https://doi.org/10.1016/j.humpath.2010.03.015>
- Artavanis-Tsakonas S, Rand MD, Lake RJ. 1999. Notch signaling: cell fate control and signal integration in development. *Science* **284**:770–776. DOI: <https://doi.org/10.1126/science.284.5415.770>, PMID: 10221902
- Baonza A, de Celis JF, García-Bellido A. 2000. Relationships between extramacrochaetae and Notch signalling in *Drosophila* wing development. *Development* **127**:2383–2393. PMID: 10804180
- Baron M. 2012. Endocytic routes to notch activation. *Seminars in Cell & Developmental Biology* **23**:437–442. DOI: <https://doi.org/10.1016/j.semcdb.2012.01.008>, PMID: 22285298
- Belenkaya TY, Wu Y, Tang X, Zhou B, Cheng L, Sharma YV, Yan D, Selva EM, Lin X. 2008. The retromer complex influences Wnt secretion by recycling Wntless from endosomes to the trans-Golgi network. *Developmental Cell* **14**:120–131. DOI: <https://doi.org/10.1016/j.devcel.2007.12.003>, PMID: 18160348
- Bertet C, Li X, Erlik T, Cavey M, Wells B, Desplan C. 2014. Temporal patterning of neuroblasts controls Notch-mediated cell survival through regulation of hid or reaper. *Cell* **158**:1173–1186. DOI: <https://doi.org/10.1016/j.cell.2014.07.045>, PMID: 25171415
- Blanpain C, Lowry WE, Pasolli HA, Fuchs E. 2006. Canonical notch signaling functions as a commitment switch in the epidermal lineage. *Genes & Development* **20**:3022–3035. DOI: <https://doi.org/10.1101/gad.1477606>
- Bowman SK, Rolland V, Betschinger J, Kinsey KA, Emery G, Knoblich JA. 2008. The tumor suppressors brat and numb regulate transit-amplifying neuroblast lineages in *Drosophila*. *Developmental Cell* **14**:535–546. DOI: <https://doi.org/10.1016/j.devcel.2008.03.004>, PMID: 18342578
- Brand AH, Livesey FJ. 2011. Neural stem cell biology in vertebrates and invertebrates: more alike than different? *Neuron* **70**:719–729. DOI: <https://doi.org/10.1016/j.neuron.2011.05.016>, PMID: 21609827
- Bray SJ. 2006. Notch signalling: a simple pathway becomes complex. *Nature Reviews Molecular Cell Biology* **7**:678–689. DOI: <https://doi.org/10.1038/nrm2009>
- Bredel M, Bredel C, Juric D, Harsh GR, Vogel H, Recht LD, Sikic BI. 2005. Functional network analysis reveals extended gliomagenesis pathway maps and three novel MYC-interacting genes in human gliomas. *Cancer Research* **65**:8679–8689. DOI: <https://doi.org/10.1158/0008-5472.CAN-05-1204>, PMID: 16204036
- Bu P, Wang L, Chen KY, Srinivasan T, Murthy PK, Tung KL, Varanko AK, Chen HJ, Ai Y, King S, Lipkin SM, Shen X. 2016. A miR-34a-Numb feedforward loop triggered by inflammation regulates asymmetric stem cell division in intestine and colon cancer. *Cell Stem Cell* **18**:189–202. DOI: <https://doi.org/10.1016/j.stem.2016.01.006>, PMID: 26849305
- Bultje RS, Castaneda-Castellanos DR, Jan LY, Jan YN, Kriegstein AR, Shi SH. 2009. Mammalian Par3 regulates progenitor cell asymmetric division via notch signaling in the developing neocortex. *Neuron* **63**:189–202. DOI: <https://doi.org/10.1016/j.neuron.2009.07.004>, PMID: 19640478
- Burd C, Cullen PJ. 2014. Retromer: a master conductor of endosome sorting. *Cold Spring Harbor Perspectives in Biology* **6**:a016774. DOI: <https://doi.org/10.1101/cshperspect.a016774>, PMID: 24492709
- Caussin E, Gonzalez C. 2005. Induction of tumor growth by altered stem-cell asymmetric division in *Drosophila melanogaster*. *Nature Genetics* **37**:1125–1129. DOI: <https://doi.org/10.1038/ng1632>
- Chen D, Xiao H, Zhang K, Wang B, Gao Z, Jian Y, Qi X, Sun J, Miao L, Yang C. 2010. Retromer is required for apoptotic cell clearance by phagocytic receptor recycling. *Science* **327**:1261–1264. DOI: <https://doi.org/10.1126/science.1184840>, PMID: 20133524
- Chen Z, Del Valle Rodriguez A, Li X, Erlik T, Fernandes VM, Desplan C. 2016. A unique class of neural progenitors in the *Drosophila* optic lobe generates both migrating neurons and Glia. *Cell Reports* **15**:774–786. DOI: <https://doi.org/10.1016/j.celrep.2016.03.061>, PMID: 27149843
- Childress JL, Acar M, Tao C, Halder G. 2006. Lethal giant discs, a novel C2-domain protein, restricts Notch activation during endocytosis. *Current Biology* **16**:2228–2233. DOI: <https://doi.org/10.1016/j.cub.2006.09.031>, PMID: 17088062
- Choy RW, Park M, Temkin P, Herring BE, Marley A, Nicoll RA, von Zastrow M. 2014. Retromer mediates a discrete route of local membrane delivery to dendrites. *Neuron* **82**:55–62. DOI: <https://doi.org/10.1016/j.neuron.2014.02.018>, PMID: 24698268
- Conboy IM, Rando TA. 2002. The regulation of Notch signaling controls satellite cell activation and cell fate determination in postnatal myogenesis. *Developmental Cell* **3**:397–409. DOI: [https://doi.org/10.1016/S1534-5807\(02\)00254-X](https://doi.org/10.1016/S1534-5807(02)00254-X), PMID: 12361602
- Cornell M, Evans DA, Mann R, Fostier M, Flasz M, Monthatong M, Artavanis-Tsakonas S, Baron M. 1999. The *Drosophila* *Melanogaster* suppressor of deltex gene, a regulator of the Notch receptor signaling pathway, is an E3 class ubiquitin ligase. *Genetics* **152**:567–576. PMID: 10353900
- Coudreuse DY, Roël G, Betist MC, Destrée O, Korswagen HC. 2006. Wnt gradient formation requires retromer function in Wnt-producing cells. *Science* **312**:921–924. DOI: <https://doi.org/10.1126/science.1124856>, PMID: 16645052
- Coumilleau F, Fürthauer M, Knoblich JA, González-Gaitán M. 2009. Directional Delta and Notch trafficking in *sara* endosomes during asymmetric cell division. *Nature* **458**:1051–1055. DOI: <https://doi.org/10.1038/nature07854>, PMID: 19295516
- Couturier L, Vodovar N, Schweisguth F. 2012. Endocytosis by numb breaks Notch symmetry at cytokinesis. *Nature Cell Biology* **14**:131–139. DOI: <https://doi.org/10.1038/ncb2419>, PMID: 22267085
- Dalton HE, Denton D, Foot NJ, Ho K, Mills K, Brou C, Kumar S. 2011. *Drosophila* Ndfip is a novel regulator of Notch signaling. *Cell Death & Differentiation* **18**:1150–1160. DOI: <https://doi.org/10.1038/cdd.2010.130>, PMID: 20966964

- Demitrack ES**, Gifford GB, Keeley TM, Carulli AJ, VanDussen KL, Thomas D, Giordano TJ, Liu Z, Kopan R, Samuelson LC. 2015. Notch signaling regulates gastric antral LGR5 stem cell function. *The EMBO Journal* **34**: 2522–2536. DOI: <https://doi.org/10.15252/embj.201490583>
- Dong Z**, Yang N, Yeo SY, Chitnis A, Guo S. 2012. Intralineage directional notch signaling regulates self-renewal and differentiation of asymmetrically dividing radial Glia. *Neuron* **74**:65–78. DOI: <https://doi.org/10.1016/j.neuron.2012.01.031>, PMID: 22500631
- Eroglu E**, Burkard TR, Jiang Y, Saini N, Homem CCF, Reichert H, Knoblich JA. 2014. SWI/SNF complex prevents lineage reversion and induces temporal patterning in neural stem cells. *Cell* **156**:1259–1273. DOI: <https://doi.org/10.1016/j.cell.2014.01.053>, PMID: 24630726
- Evans CJ**, Olson JM, Ngo KT, Kim E, Lee NE, Kuoy E, Patananan AN, Sitz D, Tran P, Do M-T, Yackle K, Cespedes A, Hartenstein V, Call GB, Banerjee U. 2009. G-TRACE: rapid Gal4-based cell lineage analysis in Drosophila. *Nature Methods* **6**:603–605. DOI: <https://doi.org/10.1038/nmeth.1356>
- Flores GV**, Duan H, Yan H, Nagaraj R, Fu W, Zou Y, Noll M, Banerjee U. 2000. Combinatorial signaling in the specification of unique cell fates. *Cell* **103**:75–85. DOI: [https://doi.org/10.1016/S0092-8674\(00\)00106-9](https://doi.org/10.1016/S0092-8674(00)00106-9), PMID: 11051549
- Franch-Marro X**, Wendler F, Guidato S, Griffith J, Baena-Lopez A, Itasaki N, Maurice MM, Vincent JP. 2008. Wingless secretion requires endosome-to-Golgi retrieval of Wntless/Evi/Sprinter by the retromer complex. *Nature Cell Biology* **10**:170–177. DOI: <https://doi.org/10.1038/ncb1678>, PMID: 18193037
- Fre S**, Huyghe M, Mourikis P, Robine S, Louvard D, Artavanis-Tsakonas S. 2005. Notch signals control the fate of immature progenitor cells in the intestine. *Nature* **435**:964–968. DOI: <https://doi.org/10.1038/nature03589>
- Froldi F**, Szuperak M, Weng C-F, Shi W, Papenfuss AT, Cheng LY. 2015. The transcription factor Nerfin-1 prevents reversion of neurons into neural stem cells. *Genes & Development* **29**:129–143. DOI: <https://doi.org/10.1101/gad.250282.114>
- Gallagher CM**, Knoblich JA. 2006. The conserved C2 domain protein lethal (2) giant discs regulates protein trafficking in Drosophila. *Developmental Cell* **11**:641–653. DOI: <https://doi.org/10.1016/j.devcel.2006.09.014>, PMID: 17084357
- George RM**, Biressi S, Beres BJ, Rogers E, Mulia AK, Allen RE, Rawls A, Rando TA, Wilson-Rawls J. 2013. Numb-deficient satellite cells have regeneration and proliferation defects. *PNAS* **110**:18549–18554. DOI: <https://doi.org/10.1073/pnas.1311628110>
- Giebel B**, Wodarz A. 2006. Tumor suppressors: control of signaling by endocytosis. *Current Biology* **16**:R91–R92. DOI: <https://doi.org/10.1016/j.cub.2006.01.022>, PMID: 16461271
- Gomez-Lamarca MJ**, Snowdon LA, Seib E, Klein T, Bray SJ. 2015. Rme-8 depletion perturbs Notch recycling and predisposes to pathogenic signaling. *The Journal of Cell Biology* **210**:303–318. DOI: <https://doi.org/10.1083/jcb.201411001>
- Gunage RD**, Reichert H, VijayRaghavan K. 2014. Identification of a new stem cell population that generates Drosophila flight muscles. *eLife* **3**:e03126. DOI: <https://doi.org/10.7554/eLife.03126>
- Guo Z**, Ohlstein B. 2015. Bidirectional Notch signaling regulates Drosophila intestinal stem cell multipotency. *Science* **350**:aab0988. DOI: <https://doi.org/10.1126/science.aab0988>
- Gupta-Rossi N**, Six E, LeBail O, Logeat F, Chastagner P, Olry A, Israël A, Brou C. 2004. Monoubiquitination and endocytosis direct γ -secretase cleavage of activated Notch receptor. *The Journal of Cell Biology* **166**:73–83. DOI: <https://doi.org/10.1083/jcb.200310098>
- Harterink M**, Port F, Lorenowicz MJ, McGough IJ, Silhankova M, Betist MC, van Weering JRT, van Heesbeen RGHP, Middelkoop TC, Basler K, Cullen PJ, Korswagen HC. 2011. A SNX3-dependent retromer pathway mediates retrograde transport of the Wnt sorting receptor Wntless and is required for Wnt secretion. *Nature Cell Biology* **13**:914–923. DOI: <https://doi.org/10.1038/ncb2281>
- Hesketh GG**, Pérez-Dorado I, Jackson LP, Wartosch L, Schäfer IB, Gray SR, McCoy AJ, Zeldin OB, Garman EF, Harbour ME, Evans PR, Seaman MNJ, Luzio JP, Owen DJ. 2014. VARP is recruited on to endosomes by direct interaction with retromer, where together they function in export to the cell surface. *Developmental Cell* **29**: 591–606. DOI: <https://doi.org/10.1016/j.devcel.2014.04.010>, PMID: 24856514
- Hilton MJ**, Tu X, Wu X, Bai S, Zhao H, Kobayashi T, Kronenberg HM, Teitelbaum SL, Ross FP, Kopan R, Long F. 2008. Notch signaling maintains bone marrow mesenchymal progenitors by suppressing osteoblast differentiation. *Nature Medicine* **14**:306–314. DOI: <https://doi.org/10.1038/nm1716>
- Homem CCF**, Knoblich JA. 2012. Drosophila neuroblasts: a model for stem cell biology. *Development* **139**:4297–4310. DOI: <https://doi.org/10.1242/dev.080515>
- Hori K**, Sen A, Kirchhausen T, Artavanis-Tsakonas S. 2011. Synergy between the ESCRT-III complex and Deltex defines a ligand-independent Notch signal. *The Journal of Cell Biology* **195**:1005–1015. DOI: <https://doi.org/10.1083/jcb.201104146>
- Horner DS**, Pasini ME, Beltrame M, Mastrodonato V, Morelli E, Vaccari T. 2018. ESCRT genes and regulation of developmental signaling. *Seminars in Cell & Developmental Biology* **74**:29–39. DOI: <https://doi.org/10.1016/j.semcdb.2017.08.038>
- Huppert SS**, Jacobsen TL, Muskavitch MA. 1997. Feedback regulation is central to Delta-Notch signalling required for Drosophila wing vein morphogenesis. *Development* **124**:3283–3291.
- Hutterer A**, Knoblich JA. 2005. Numb and α -Adaptin regulate sanpodo endocytosis to specify cell fate in Drosophila external sensory organs. *EMBO Reports* **6**:836–842. DOI: <https://doi.org/10.1038/sj.embor.7400500>, PMID: 16113648

- Jaekel R, Klein T.** 2006. The Drosophila notch inhibitor and tumor suppressor gene lethal (2) giant discs encodes a conserved regulator of endosomal trafficking. *Developmental Cell* **11**:655–669. DOI: <https://doi.org/10.1016/j.devcel.2006.09.019>, PMID: 17084358
- Knoblich JA.** 2010. Asymmetric cell division: recent developments and their implications for tumour biology. *Nature Reviews Molecular Cell Biology* **11**:849–860. DOI: <https://doi.org/10.1038/nrm3010>
- Kopan R, Ilagan MX.** 2009. The canonical notch signaling pathway: unfolding the activation mechanism. *Cell* **137**: 216–233. DOI: <https://doi.org/10.1016/j.cell.2009.03.045>, PMID: 19379690
- Kopan R.** 2012. Notch signaling. *Cold Spring Harbor Perspectives in Biology* **4**:a011213. DOI: <https://doi.org/10.1101/cshperspect.a011213>, PMID: 23028119
- Kressmann S, Campos C, Castanon I, Fürthauer M, González-Gaitán M.** 2015. Directional Notch trafficking in sara endosomes during asymmetric cell division in the spinal cord. *Nature Cell Biology* **17**:333–339. DOI: <https://doi.org/10.1038/ncb3119>, PMID: 25706234
- Lah JJ, Levey AI.** 2000. Endogenous presenilin-1 targets to endocytic rather than biosynthetic compartments. *Molecular and Cellular Neuroscience* **16**:111–126. DOI: <https://doi.org/10.1006/mcne.2000.0861>, PMID: 10924255
- Landskron L, Steinmann V, Bonnay F, Burkard TR, Steinmann J, Reichardt I, Harzer H, Laurenson AS, Reichert H, Knoblich JA.** 2018. The asymmetrically segregating lncRNA cherub is required for transforming stem cells into malignant cells. *eLife* **7**:e31347. DOI: <https://doi.org/10.7554/eLife.31347>, PMID: 29580384
- Le Bras S, Loyer N, Le Borgne R.** 2011. The multiple facets of ubiquitination in the regulation of notch signaling pathway. *Traffic* **12**:149–161. DOI: <https://doi.org/10.1111/j.1600-0854.2010.01126.x>, PMID: 21029288
- Lee C-Y, Andersen RO, Cabernard C, Manning L, Tran KD, Lanskey MJ, Bashirullah A, Doe CQ.** 2006a. Drosophila Aurora-A kinase inhibits neuroblast self-renewal by regulating aPKC/Numb cortical polarity and spindle orientation. *Genes & Development* **20**:3464–3474. DOI: <https://doi.org/10.1101/gad.1489406>
- Lee J, Kotliarova S, Kotliarov Y, Li A, Su Q, Donin NM, Pastorino S, Puro BW, Christopher N, Zhang W, Park JK, Fine HA.** 2006b. Tumor stem cells derived from glioblastomas cultured in bFGF and EGF more closely mirror the phenotype and genotype of primary tumors than do serum-cultured cell lines. *Cancer Cell* **9**:391–403. DOI: <https://doi.org/10.1016/j.ccr.2006.03.030>
- Lee T, Luo L.** 1999. Mosaic analysis with a repressible cell marker for studies of gene function in neuronal morphogenesis. *Neuron* **22**:451–461. DOI: [https://doi.org/10.1016/S0896-6273\(00\)80701-1](https://doi.org/10.1016/S0896-6273(00)80701-1), PMID: 10197526
- Li HS, Wang D, Shen Q, Schonemann MD, Gorski JA, Jones KR, Temple S, Jan LY, Jan YN.** 2003. Inactivation of numb and numblike in embryonic dorsal forebrain impairs neurogenesis and disrupts cortical morphogenesis. *Neuron* **40**:1105–1118. DOI: [https://doi.org/10.1016/S0896-6273\(03\)00755-4](https://doi.org/10.1016/S0896-6273(03)00755-4), PMID: 14687546
- Lieber T, Kidd S, Young MW.** 2002. kuzbanian-mediated cleavage of Drosophila Notch. *Genes & Development* **16**:209–221. DOI: <https://doi.org/10.1101/gad.942302>
- Lin S, Kao CF, Yu HH, Huang Y, Lee T.** 2012. Lineage analysis of Drosophila lateral antennal lobe neurons reveals notch-dependent binary temporal fate decisions. *PLoS Biology* **10**:e1001425. DOI: <https://doi.org/10.1371/journal.pbio.1001425>, PMID: 23185131
- Liu J, Sato C, Cerletti M, Wagers A.** 2010. Notch signaling in the regulation of stem cell self-renewal and differentiation. *Current Topics in Developmental Biology* **92**:367–409. DOI: [https://doi.org/10.1016/S0070-2153\(10\)92012-7](https://doi.org/10.1016/S0070-2153(10)92012-7), PMID: 20816402
- Liu K, Shen D, Shen J, Gao SM, Li B, Wong C, Feng W, Song Y.** 2017. The super elongation complex drives neural stem cell fate commitment. *Developmental Cell* **40**:537–551. DOI: <https://doi.org/10.1016/j.devcel.2017.02.022>, PMID: 28350987
- Lloyd TE, Atkinson R, Wu MN, Zhou Y, Pennetta G, Bellen HJ.** 2002. Hrs regulates endosome membrane invagination and tyrosine kinase receptor signaling in Drosophila. *Cell* **108**:261–269. DOI: [https://doi.org/10.1016/S0092-8674\(02\)00611-6](https://doi.org/10.1016/S0092-8674(02)00611-6), PMID: 11832215
- Losick R, Desplan C.** 2008. Stochasticity and cell fate. *Science* **320**:65–68. DOI: <https://doi.org/10.1126/science.1147888>, PMID: 18388284
- Lu B, Rothenberg M, Jan LY, Jan YN.** 1998. Partner of numb colocalizes with numb during mitosis and directs numb asymmetric localization in Drosophila neural and muscle progenitors. *Cell* **95**:225–235. DOI: [https://doi.org/10.1016/S0092-8674\(00\)81753-5](https://doi.org/10.1016/S0092-8674(00)81753-5), PMID: 9790529
- Luo D, Renault VM, Rando TA.** 2005. The regulation of Notch signaling in muscle stem cell activation and postnatal myogenesis. *Seminars in Cell & Developmental Biology* **16**:612–622. DOI: <https://doi.org/10.1016/j.semcdb.2005.07.002>
- Luo L, Liao YJ, Jan LY, Jan YN.** 1994. Distinct morphogenetic functions of similar small GTPases: Drosophila Drac1 is involved in axonal outgrowth and myoblast fusion. *Genes & Development* **8**:1787–1802. DOI: <https://doi.org/10.1101/gad.8.15.1787>
- McMillan KJ, Korswagen HC, Cullen PJ.** 2017. The emerging role of retromer in neuroprotection. *Current Opinion in Cell Biology* **47**:72–82. DOI: <https://doi.org/10.1016/j.ceb.2017.02.004>
- Monastirioti M, Giagtzoglou N, Koumbanakis KA, Zacharioudaki E, Deligiannaki M, Wech I, Almeida M, Preiss A, Bray S, Delidakis C.** 2010. Drosophila hey is a target of Notch in asymmetric divisions during embryonic and larval neurogenesis. *Development* **137**:191–201. DOI: <https://doi.org/10.1242/dev.043604>, PMID: 20040486
- Mukherjee T, Kim WS, Mandal L, Banerjee U.** 2011. Interaction between notch and Hif-alpha in development and survival of Drosophila blood cells. *Science* **332**:1210–1213. DOI: <https://doi.org/10.1126/science.1199643>, PMID: 21636775

- Mumm JS**, Schroeter EH, Saxena MT, Griesemer A, Tian X, Pan DJ, Ray WJ, Kopan R. 2000. A ligand-induced extracellular cleavage regulates gamma-secretase-like proteolytic activation of Notch1. *Molecular Cell* **5**:197–206. DOI: [https://doi.org/10.1016/S1097-2765\(00\)80416-5](https://doi.org/10.1016/S1097-2765(00)80416-5), PMID: 10882062
- Mund T**, Pelham HR. 2009. Control of the activity of WW-HECT domain E3 ubiquitin ligases by NDFIP proteins. *EMBO Reports* **10**:501–507. DOI: <https://doi.org/10.1038/embor.2009.30>, PMID: 19343052
- Narbonne-Reveau K**, Lanet E, Dillard C, Foppolo S, Chen CH, Parrinello H, Rialle S, Sokol NS, Maurice C. 2016. Neural stem cell-encoded temporal patterning delineates an early window of malignant susceptibility in *Drosophila*. *eLife* **5**:e13463. DOI: <https://doi.org/10.7554/eLife.13463>, PMID: 27296804
- O'Connor-Giles KM**, Skeath JB. 2003. Numb inhibits membrane localization of Sanpodo, a four-pass transmembrane protein, to promote asymmetric divisions in *Drosophila*. *Developmental Cell* **5**:231–243. DOI: [https://doi.org/10.1016/S1534-5807\(03\)00226-0](https://doi.org/10.1016/S1534-5807(03)00226-0), PMID: 12919675
- Ohlstein B**, Spradling A. 2007. Multipotent *Drosophila* intestinal stem cells specify daughter cell fates by differential notch signaling. *Science* **315**:988–992. DOI: <https://doi.org/10.1126/science.1136606>, PMID: 17303754
- Palmer WH**, Deng WM. 2015. Ligand-independent mechanisms of notch activity. *Trends in Cell Biology* **25**:697–707. DOI: <https://doi.org/10.1016/j.tcb.2015.07.010>, PMID: 26437585
- Pan CL**, Baum PD, Gu M, Jorgensen EM, Clark SG, Garriga G. 2008. *C. elegans* AP-2 and retromer control Wnt signaling by regulating mig-14/Wntless. *Developmental Cell* **14**:132–139. DOI: <https://doi.org/10.1016/j.devcel.2007.12.001>, PMID: 18160346
- Pan D**, Rubin GM. 1997. Kuzbanian controls proteolytic processing of notch and mediates lateral inhibition during *Drosophila* and vertebrate neurogenesis. *Cell* **90**:271–280. DOI: [https://doi.org/10.1016/S0092-8674\(00\)80335-9](https://doi.org/10.1016/S0092-8674(00)80335-9), PMID: 9244301
- Pasternak SH**, Bagshaw RD, Guiral M, Zhang S, Ackerley CA, Pak BJ, Callahan JW, Mahuran DJ. 2003. Presenilin-1, Nicastrin, amyloid precursor protein, and γ -secretase activity are co-localized in the lysosomal membrane. *Journal of Biological Chemistry* **278**:26687–26694. DOI: <https://doi.org/10.1074/jbc.M304009200>, PMID: 12736250
- Pece S**, Serresi M, Santolini E, Capra M, Hulleman E, Galimberti V, Zurrada S, Maisonneuve P, Viale G, Di Fiore PP. 2004. Loss of negative regulation by Numb over Notch is relevant to human breast carcinogenesis. *The Journal of Cell Biology* **167**:215–221. DOI: <https://doi.org/10.1083/jcb.200406140>
- Pfeiffer BD**, Jenett A, Hammonds AS, Ngo T-TB, Misra S, Murphy C, Scully A, Carlson JW, Wan KH, Lavery TR, Mungall C, Svirskas R, Kadonaga JT, Doe CQ, Eisen MB, Celniker SE, Rubin GM. 2008. Tools for neuroanatomy and neurogenetics in *Drosophila*. *PNAS* **105**:9715–9720. DOI: <https://doi.org/10.1073/pnas.0803697105>
- Pinto-Teixeira F**, Koo C, Rossi AM, Neriec N, Bertet C, Li X, Del-Valle-Rodriguez A, Desplan C. 2018. Development of concurrent retinotopic maps in the fly motion detection circuit. *Cell* **173**:485–498. DOI: <https://doi.org/10.1016/j.cell.2018.02.053>, PMID: 29576455
- Pocha SM**, Wassmer T, Niehage C, Hoflack B, Knust E. 2011. Retromer controls epithelial cell polarity by trafficking the apical determinant crumbs. *Current Biology* **21**:1111–1117. DOI: <https://doi.org/10.1016/j.cub.2011.05.007>, PMID: 21700461
- Port F**, Kuster M, Herr P, Furger E, Bänziger C, Hausmann G, Basler K. 2008. Wingless secretion promotes and requires retromer-dependent cycling of Wntless. *Nature Cell Biology* **10**:178–185. DOI: <https://doi.org/10.1038/ncb1687>, PMID: 18193032
- Qiu L**, Joazeiro C, Fang N, Wang HY, Ely C, Altman Y, Fang D, Hunter T, Liu YC. 2000. Recognition and ubiquitination of notch by itch, a hect-type E3 ubiquitin ligase. *Journal of Biological Chemistry* **275**:35734–35737. DOI: <https://doi.org/10.1074/jbc.M007300200>, PMID: 10940313
- Ren Q**, Awasaki T, Wang Y-C, Huang Y-F, Lee T. 2018. Lineage-guided Notch-dependent gliogenesis by *Drosophila* multi-potent progenitors. *Development* **145**:dev160127. DOI: <https://doi.org/10.1242/dev.160127>
- Rhyu MS**, Jan LY, Jan YN. 1994. Asymmetric distribution of numb protein during division of the sensory organ precursor cell confers distinct fates to daughter cells. *Cell* **76**:477–491. DOI: [https://doi.org/10.1016/0092-8674\(94\)90112-0](https://doi.org/10.1016/0092-8674(94)90112-0)
- Rossi F**, Gonzalez C. 2015. Studying tumor growth in *Drosophila* using the tissue allograft method. *Nature Protocols* **10**:1525–1534. DOI: <https://doi.org/10.1038/nprot.2015.096>, PMID: 26357008
- Sakata T**, Sakaguchi H, Tsuda L, Higashitani A, Aigaki T, Matsuno K, Hayashi S. 2004. *Drosophila* Nedd4 regulates endocytosis of Notch and suppresses its ligand-independent activation. *Current Biology* **14**:2228–2236. DOI: <https://doi.org/10.1016/j.cub.2004.12.028>, PMID: 15620649
- Sallé J**, Gervais L, Boumard B, Stefanutti M, Siudeja K, Bardin AJ. 2017. Intrinsic regulation of enteroendocrine fate by numb. *The EMBO Journal* **36**:1928–1945. DOI: <https://doi.org/10.15252/embj.201695622>, PMID: 28533229
- Schneider M**, Troost T, Grawe F, Martinez-Arias A, Klein T. 2013. Activation of Notch in Igd mutant cells requires the fusion of late endosomes with the lysosome. *Journal of Cell Science* **126**:645–656. DOI: <https://doi.org/10.1242/jcs.116590>, PMID: 23178945
- Shen Q**, Zhong W, Jan YN, Temple S. 2002. Asymmetric numb distribution is critical for asymmetric cell division of mouse cerebral cortical stem cells and neuroblasts. *Development* **129**:4843–4853. PMID: 12361975
- Small SA**, Gandy S. 2006. Sorting through the cell biology of Alzheimer's disease: intracellular pathways to pathogenesis. *Neuron* **52**:15–31. DOI: <https://doi.org/10.1016/j.neuron.2006.09.001>, PMID: 17015224
- Small SA**, Petsko GA. 2015. Retromer in alzheimer disease, parkinson disease and other neurological disorders. *Nature Reviews Neuroscience* **16**:126–132. DOI: <https://doi.org/10.1038/nrn3896>, PMID: 25669742

- Song Y**, Lu B. 2011. Regulation of cell growth by Notch signaling and its differential requirement in normal vs. tumor-forming stem cells in *Drosophila*. *Genes & Development* **25**:2644–2658. DOI: <https://doi.org/10.1101/gad.171959.111>, PMID: 22190460
- Song Y**, Lu B. 2012. Interaction of notch signaling modulator numb with α -Adaptin regulates endocytosis of notch pathway components and cell fate determination of neural stem cells. *Journal of Biological Chemistry* **287**:17716–17728. DOI: <https://doi.org/10.1074/jbc.M112.360719>, PMID: 22474327
- Sousa-Nunes R**, Cheng LY, Gould AP. 2010. Regulating neural proliferation in the *Drosophila* CNS. *Current Opinion in Neurobiology* **20**:50–57. DOI: <https://doi.org/10.1016/j.conb.2009.12.005>, PMID: 20079625
- Starble R**, Pokrywka NJ. 2018. The retromer subunit Vps26 mediates Notch signaling during *Drosophila* oogenesis. *Mechanisms of Development* **149**:1–8. DOI: <https://doi.org/10.1016/j.mod.2017.10.001>, PMID: 29031909
- Tanaka T**, Nakamura A. 2008. The endocytic pathway acts downstream of Oskar in *Drosophila* germ plasm assembly. *Development* **135**:1107–1117. DOI: <https://doi.org/10.1242/dev.017293>, PMID: 18272590
- Temkin P**, Lauffer B, Jäger S, Cimermancic P, Krogan NJ, von Zastrow M. 2011. SNX27 mediates retromer tubule entry and endosome-to-plasma membrane trafficking of signalling receptors. *Nature Cell Biology* **13**:715–721. DOI: <https://doi.org/10.1038/ncb2252>, PMID: 21602791
- Temkin P**, Morishita W, Goswami D, Arendt K, Chen L, Malenka R. 2017. The retromer supports AMPA receptor trafficking during LTP. *Neuron* **94**:74–82. DOI: <https://doi.org/10.1016/j.neuron.2017.03.020>, PMID: 28384478
- Thompson BJ**, Mathieu J, Sung HH, Loeser E, Rorth P, Cohen SM. 2005. Tumor suppressor properties of the ESCRT-II complex component Vps25 in *Drosophila*. *Developmental Cell* **9**:711–720. DOI: <https://doi.org/10.1016/j.devcel.2005.09.020>, PMID: 16256745
- Urta S**, Escudero CA, Ramos P, Lisbona F, Allende E, Covarrubias P, Parraguez JI, Zampieri N, Chao MV, Annaert W, Bronfman FC. 2007. TrkA receptor activation by nerve growth factor induces shedding of the p75 neurotrophin receptor followed by endosomal gamma-secretase-mediated release of the p75 intracellular domain. *Journal of Biological Chemistry* **282**:7606–7615. DOI: <https://doi.org/10.1074/jbc.M610458200>, PMID: 17215246
- Vaccari T**, Bilder D. 2005. The *Drosophila* tumor suppressor vps25 prevents nonautonomous overproliferation by regulating notch trafficking. *Developmental Cell* **9**:687–698. DOI: <https://doi.org/10.1016/j.devcel.2005.09.019>, PMID: 16256743
- Vaccari T**, Rusten TE, Menut L, Nezis IP, Brech A, Stenmark H, Bilder D. 2009. Comparative analysis of ESCRT-I, ESCRT-II and ESCRT-III function in *Drosophila* by efficient isolation of ESCRT mutants. *Journal of Cell Science* **122**:2413–2423. DOI: <https://doi.org/10.1242/jcs.046391>, PMID: 19571114
- Wang C**, Zhang W, Yin MX, Hu L, Li P, Xu J, Huang H, Wang S, Lu Y, Wu W, Ho MS, Li L, Zhao Y, Zhang L. 2015. Suppressor of deltex mediates pez degradation and modulates *Drosophila* midgut homeostasis. *Nature Communications* **6**:6607. DOI: <https://doi.org/10.1038/ncomms7607>, PMID: 25814387
- Wang H**, Somers GW, Bashirullah A, Heberlein U, Yu F, Chia W. 2006. Aurora-A acts as a tumor suppressor and regulates self-renewal of *Drosophila* neuroblasts. *Genes & Development* **20**:3453–3463. DOI: <https://doi.org/10.1101/gad.1487506>, PMID: 17182870
- Wang S**, Bellen HJ. 2015. The retromer complex in development and disease. *Development* **142**:2392–2396. DOI: <https://doi.org/10.1242/dev.123737>, PMID: 26199408
- Wang S**, Tan KL, Agosto MA, Xiong B, Yamamoto S, Sandoval H, Jaiswal M, Bayat V, Zhang K, Charng WL, David G, Duraine L, Venkatachalam K, Wensel TG, Bellen HJ. 2014. The retromer complex is required for rhodopsin recycling and its loss leads to photoreceptor degeneration. *PLoS Biology* **12**:e1001847. DOI: <https://doi.org/10.1371/journal.pbio.1001847>, PMID: 24781186
- Watt FM**, Estrach S, Ambler CA. 2008. Epidermal Notch signalling: differentiation, cancer and adhesion. *Current Opinion in Cell Biology* **20**:171–179. DOI: <https://doi.org/10.1016/j.ceb.2008.01.010>, PMID: 18342499
- Weng M**, Golden KL, Lee CY. 2010. dFzef/Earmuff maintains the restricted developmental potential of intermediate neural progenitors in *Drosophila*. *Developmental Cell* **18**:126–135. DOI: <https://doi.org/10.1016/j.devcel.2009.12.007>, PMID: 20152183
- Wilkin M**, Tongngok P, Gensch N, Clemence S, Motoki M, Yamada K, Hori K, Taniguchi-Kanai M, Franklin E, Matsuno K, Baron M. 2008. *Drosophila* HOPS and AP-3 complex genes are required for a Deltex-regulated activation of notch in the endosomal trafficking pathway. *Developmental Cell* **15**:762–772. DOI: <https://doi.org/10.1016/j.devcel.2008.09.002>, PMID: 19000840
- Wilkin MB**, Carbery AM, Fostier M, Aslam H, Mazaleyrat SL, Higgs J, Myat A, Evans DA, Cornell M, Baron M. 2004. Regulation of notch endosomal sorting and signaling by *Drosophila* Nedd4 family proteins. *Current Biology* **14**:2237–2244. DOI: <https://doi.org/10.1016/j.cub.2004.11.030>, PMID: 15620650
- Williams SE**, Beronja S, Pasolli HA, Fuchs E. 2011. Asymmetric cell divisions promote Notch-dependent epidermal differentiation. *Nature* **470**:353–358. DOI: <https://doi.org/10.1038/nature09793>, PMID: 21331036
- Wu YC**, Lee KS, Song Y, Gehrke S, Lu B. 2017. The bantam microRNA acts through Numb to exert cell growth control and feedback regulation of Notch in tumor-forming stem cells in the *Drosophila* brain. *PLoS Genetics* **13**:e1006785. DOI: <https://doi.org/10.1371/journal.pgen.1006785>, PMID: 28520736
- Xiao Q**, Komori H, Lee CY. 2012. klumpfuss distinguishes stem cells from progenitor cells during asymmetric neuroblast division. *Development* **139**:2670–2680. DOI: <https://doi.org/10.1242/dev.081687>, PMID: 22745313
- Yang PT**, Lorenowicz MJ, Silhankova M, Coudreuse DY, Betist MC, Korswagen HC. 2008. Wnt signaling requires retromer-dependent recycling of MIG-14/Wntless in Wnt-producing cells. *Developmental Cell* **14**:140–147. DOI: <https://doi.org/10.1016/j.devcel.2007.12.004>, PMID: 18160347

- Zhang Q**, Wu X, Chen P, Liu L, Xin N, Tian Y, Dillin A. 2018. The mitochondrial unfolded protein response is mediated Cell-Non-autonomously by Retromer-Dependent Wnt signaling. *Cell* **174**:870–883. DOI: <https://doi.org/10.1016/j.cell.2018.06.029>, PMID: 30057120
- Zhong W**, Feder JN, Jiang MM, Jan LY, Jan YN. 1996. Asymmetric localization of a mammalian numb homolog during mouse cortical neurogenesis. *Neuron* **17**:43–53. DOI: [https://doi.org/10.1016/S0896-6273\(00\)80279-2](https://doi.org/10.1016/S0896-6273(00)80279-2), PMID: 8755477
- Zhou W**, He Q, Zhang C, He X, Cui Z, Liu F, Li W. 2016. BLOS2 negatively regulates Notch signaling during neural and hematopoietic stem and progenitor cell development. *eLife* **5**:e18108. DOI: <https://doi.org/10.7554/eLife.18108>, PMID: 27719760
- Zhu S**, Barshow S, Wildonger J, Jan LY, Jan YN. 2011. Ets transcription factor Pointed promotes the generation of intermediate neural progenitors in Drosophila larval brains. *PNAS* **108**:20615–20620. DOI: <https://doi.org/10.1073/pnas.1118595109>, PMID: 22143802
- Zhu S**, Lin S, Kao CF, Awasaki T, Chiang AS, Lee T. 2006. Gradients of the Drosophila Chinmo BTB-zinc finger protein govern neuronal temporal identity. *Cell* **127**:409–422. DOI: <https://doi.org/10.1016/j.cell.2006.08.045>, PMID: 17055440